Cell Genomics

Article

Multivariate GWAS of psychiatric disorders and their cardinal symptoms reveal two dimensions of cross-cutting genetic liabilities

Graphical abstract

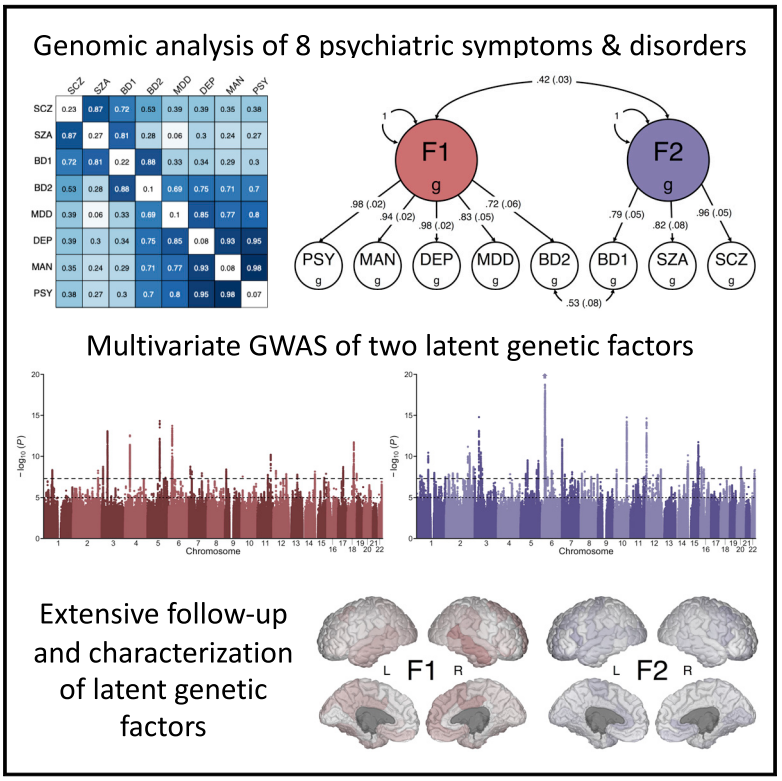

Authors

Travis T. Mallard, Richard Karlsson Linnér, Andrew D. Grotzinger, ..., Matthew C. Keller, Philipp D. Koellinger, K. Paige Harden

Correspondence

tmallard@mgh.harvard.edu (T.T.M.), harden@utexas.edu (K.P.H.)

In brief

Mallard et al. identified two transdiagnostic dimensions of genetic risk in a large genome-wide association study of psychiatric phenotypes related to mood disturbance and psychosis. While these genetic risk factors were modestly correlated, they were largely unique from one another and differed in their relationships with health and wellbeing.

Highlights

- Identification of two dimensions of genetic risk in mood and psychotic psychopathology
- Pleiotropic genes broadly implicate neuronal pathways in psychopathology
- Dimensions of genetic risk differ in their associations with health and disease

Mallard et al., 2022, Cell Genomics 2, 100140
June 8, 2022
https://doi.org/10.1016/j.xgen.2022.100140

CellPress

Cell Genomics

CellPress
OPEN ACCESS

Article

Multivariate GWAS of psychiatric disorders and their cardinal symptoms reveal two dimensions of cross-cutting genetic liabilities

Travis T. Mallard,[1,2,19,*] Richard Karlsson Linnér,[3,4] Andrew D. Grotzinger,[1] Sandra Sanchez-Roige,[5,6] Jakob Seidlitz,[7,8] Aysu Okbay,[3] Ronald de Vlaming,[3] S. Fleur W. Meddens,[9] Bipolar Disorder Working Group of the Psychiatric Genomics Consortium, Abraham A. Palmer,[5,10] Lea K. Davis,[6,11,12] Elliot M. Tucker-Drob,[1,13] Kenneth S. Kendler,[14,15] Matthew C. Keller,[16,17] Philipp D. Koellinger,[3,18] and K. Paige Harden[1,13,18,*]

[1]Department of Psychology, University of Texas at Austin, Austin, TX, USA
[2]Psychiatric and Neurodevelopmental Genetics Unit, Center for Genomic Medicine, Massachusetts General Hospital, Boston, MA, USA
[3]Department of Economics, School of Business and Economics, Vrije Universiteit Amsterdam, Amsterdam, the Netherlands
[4]Autism and Developmental Medicine Institute, Geisinger, Lewisburg, PA, USA
[5]Department of Psychiatry, University of California San Diego, La Jolla, CA, USA
[6]Department of Medicine, Vanderbilt University Medical Center, Nashville, TN, USA
[7]Department of Child and Adolescent Psychiatry and Behavioral Science, Children's Hospital of Philadelphia, Philadelphia, PA, USA
[8]Department of Psychiatry, University of Pennsylvania, Philadelphia, PA, USA
[9]Erasmus University Rotterdam Institute for Behavior and Biology, Erasmus School of Economics, Erasmus University Rotterdam, Rotterdam, the Netherlands
[10]Institute for Genomic Medicine, University of California San Diego, La Jolla, CA, USA
[11]Department of Biomedical Informatics, Vanderbilt University Medical Center, Nashville, TN, USA
[12]Department of Psychiatry and Behavioral Sciences, Vanderbilt University Medical Center, Nashville, TN, USA
[13]Population Research Center, University of Texas at Austin, Austin, TX, USA
[14]Virginia Institute for Psychiatric and Behavioral Genetics, Virginia Commonwealth University, Richmond, VA, USA
[15]Department of Psychiatry, Medical College of Virginia/Virginia Commonwealth University, Richmond, VA, USA
[16]Institute for Behavioral Genetics, University of Colorado Boulder, Boulder, CO, USA
[17]Department of Psychology and Neuroscience, University of Colorado Boulder, Boulder, CO, USA
[18]Senior author
[19]Lead contact
*Correspondence: tmallard@mgh.harvard.edu (T.T.M.), harden@utexas.edu (K.P.H.)
https://doi.org/10.1016/j.xgen.2022.100140

SUMMARY

Understanding which biological pathways are specific versus general across diagnostic categories and levels of symptom severity is critical to improving nosology and treatment of psychopathology. Here, we combine transdiagnostic and dimensional approaches to genetic discovery for the first time, conducting a novel multivariate genome-wide association study of eight psychiatric symptoms and disorders broadly related to mood disturbance and psychosis. We identify two transdiagnostic genetic liabilities that distinguish between common forms of psychopathology versus rarer forms of serious mental illness. Biological annotation revealed divergent genetic architectures that differentially implicated prenatal neurodevelopment and neuronal function and regulation. These findings inform psychiatric nosology and biological models of psychopathology, as they suggest that the severity of mood and psychotic symptoms present in serious mental illness may reflect a difference in kind rather than merely in degree.

INTRODUCTION

Psychiatric disorders are one of the leading causes of global disease burden, affecting more than 25% of the world's population at some point during their lifetime.[1] Twin- and family-based studies have established that a substantial portion of individual differences in liability to psychiatric disorders is attributable to genetic variation.[2] Genome-wide association studies (GWASs) have identified numerous genetic loci that have replicable associations with severe and debilitating psychiatric disorders, including schizophrenia,[3] bipolar disorder,[4] and major depressive disorder.[5]

GWASs have also identified a substantial degree of genetic overlap across psychiatric disorders, finding high genetic covariances and many pleiotropic loci.[6,7] This genetic overlap complicates efforts to identify causes, consequences, and treatments that are specific to any individual psychiatric disorder.[8] In response to these challenges, transdiagnostic approaches in psychiatry aim to identify biological systems that are perturbed across many forms of illness.[9,10] Transdiagnostic research may

yield new therapeutic targets with broad utility as well as inform nosological classification and stratification of at-risk populations.

Concurrent with the emergence of transdiagnostic research, efforts to identify disorder-specific genetic loci have turned toward studying self-report measures in population-based cohorts,[11–13] as case-control study designs require diagnostic schedules that can be slow and costly. If valid, this dimensional approach in non-clinical samples has the potential to accelerate genetic discovery via dramatic increases in sample size, as self-report survey measures of psychiatric symptoms can be administered at scale to large, genotyped population-based samples, such as UK Biobank.[14,15] However, while this approach may be valid for some common forms of psychopathology,[16] it is unknown whether the biology that influences normative variation in subthreshold symptoms also underlies rarer psychiatric conditions, such as those characterized by mania and/or psychosis.

Here, we combine transdiagnostic and dimensional research approaches to genetic discovery in two important ways. First, we use a novel combination of Bayesian item response theory and linear mixed models to perform GWASs of depressive (DEP), manic (MAN), and psychotic (PSY) symptoms on more than 250,000 individuals in the UK Biobank. This approach has been shown to yield higher heritability estimates than single-item measures or simple composite measures.[17,18] Second, we used genomic structural equation modeling (Genomic SEM)[19] to characterize the shared genetic architecture among these three symptom dimensions and five additional psychiatric disorders: major depressive disorder (MDD), bipolar II disorder (BD2), bipolar I disorder (BD1), schizoaffective disorder (SZA), and schizophrenia (SCZ).

These analyses yield insight into three conceptual questions in the biological study of psychopathology. First, how do the genetic bases of mood and psychotic symptoms compare and contrast with the genetic bases of psychiatric diagnoses that are characterized by those symptoms? Second, to what extent can the shared genetic architecture of these symptoms and disorders be summarized with a single dimension of liability, a "*p* factor," as has been previously proposed on the basis of phenotypic analyses?[20] Third, how are dimensions of transdiagnostic liability similar and dissimilar in their genetic architecture, underlying biology, and associations with other aspects of human wellbeing and disease?

RESULTS

Novel loci associated with lifetime endorsement of mood and psychotic symptoms

We used a combination of Bayesian item response theory and linear mixed models to conduct univariate GWASs for self-reported measures of lifetime depression, mania, and psychosis from 252,252 individuals in the UK Biobank. We observed substantial inflation of the median test statistic for all three phenotypes, and the linkage disequilibrium (LD) score regression intercepts and attenuation ratios suggest that test-statistic inflation is primarily due to polygenic signal rather than bias (Figure 1; Table 1). After applying a standard clumping algorithm via FUMA (r^2 = 0.1, 250 kb merge window), we identified 23 independent loci associated with lifetime depressive, manic, and/or psychotic symptoms (Tables S1A–S1C). Nine of these loci were significantly associated with two or more phenotypes, and six loci were associated with all three psychiatric phenotypes.

The identified risk loci span 12 chromosomes and include variants tagging the major histocompatibility complex region on chromosome 6 as well a well-known inversion polymorphism on chromosome 17 previously associated with several psychiatric phenotypes.[22] Many of these risk loci replicated previous findings from GWASs of psychopathology or were in high LD with previous hits for phenotypes including neuroticism[23] (e.g., rs7111031, rs10503002, rs4245154), broadly defined depression[11] (e.g., rs9586, rs191800971, rs7111031), and schizophrenia[24] (e.g., rs4245154, rs4702). However, several loci contained lead SNPs that were new GWAS signals altogether, identifying new regions of the genome that confer risk for psychopathology, such as rs4722389, rs7324564, and rs570217967.

Moreover, our gene-based association analyses performed via MAGMA identified 124 genes associated with at least one of the psychiatric symptoms (depression, mania, or psychosis), 31 of which were associated with all three. For all phenotypes, we observed enriched expression in brain tissue as well as an enriched signal for brain-related gene sets. We report detailed biological annotation (e.g., gene mapping, gene set enrichment, tissue enrichment) for each of these GWASs in Tables S1D–S1L.

Two transdiagnostic genetic liabilities underlie mood and psychotic psychopathology

To describe the genomic relationships among psychiatric symptoms and disorders commonly characterized by depression, mania, and/or psychosis[4,5,21] (see Table 1 for overview of study phenotypes), we first used bivariate LD score regression to estimate genetic correlations between all pairs of psychiatric phenotypes. While we observed very large positive genetic correlations among the three psychiatric symptoms (mean r_g = 0.95, SEM = 0.02), we observed more modest genetic correlations for the five psychiatric disorders (mean r_g = 0.55, SEM = 0.09). We found that schizophrenia, schizoaffective disorder, and bipolar I were highly correlated with one another ($r_{gSCZ\text{-}SZA}$ = 0.87 [SE = 0.13], $r_{gSCZ\text{-}BD1}$ = 0.72 [SE = 0.03], $r_{gSZA\text{-}BD1}$ = 0.81 [SE = 0.12]), but these disorders generally had markedly smaller genetic correlations with bipolar II and major depressive disorder ($r_{gSCZ\text{-}BD2}$ = 0.53 [SE = 0.03], $r_{gSCZ\text{-}MDD}$ = 0.39 [SE = 0.04], $r_{gSZA\text{-}BD2}$ = 0.28 [SE = 0.21], $r_{gSZA\text{-}MDD}$ = 0.06 [SE = 0.12], $r_{gBD1\text{-}MDD}$ = 0.33 [SE = 0.04]). Bipolar I and bipolar II were highly correlated, though ($r_{gBD1\text{-}BD2}$ = 0.88 [SE = 0.11]). Interestingly, we found that bipolar II and major depressive disorder were also highly correlated with each other ($r_{gBD2\text{-}MDD}$ = 0.69 [SE = 0.13]) as well as with all psychiatric symptoms ($r_{gBD2\text{-}DEP}$ = 0.75 [SE = 0.11], $r_{gBD2\text{-}MAN}$ = 0.71 [SE = 0.11], $r_{gBD2\text{-}PSY}$ = 0.70 [SE = 0.11], $r_{gMDD\text{-}DEP}$ = 0.85 [SE = 0.03], $r_{gMDD\text{-}MAN}$ = 0.77 [SE = 0.03], $r_{gMDD\text{-}PSY}$ = 0.80 [SE = 0.04]). Notably, many of these genetic correlations differed from the phenotypic correlations observed in UK Biobank (Figure S1).

After applying a hierarchical-clustering algorithm to the genetic-correlation matrix, we found two distinct clusters of psychiatric phenotypes (Figure 2A). The first cluster comprised the three psychiatric symptoms, major depressive disorder, and bipolar II,

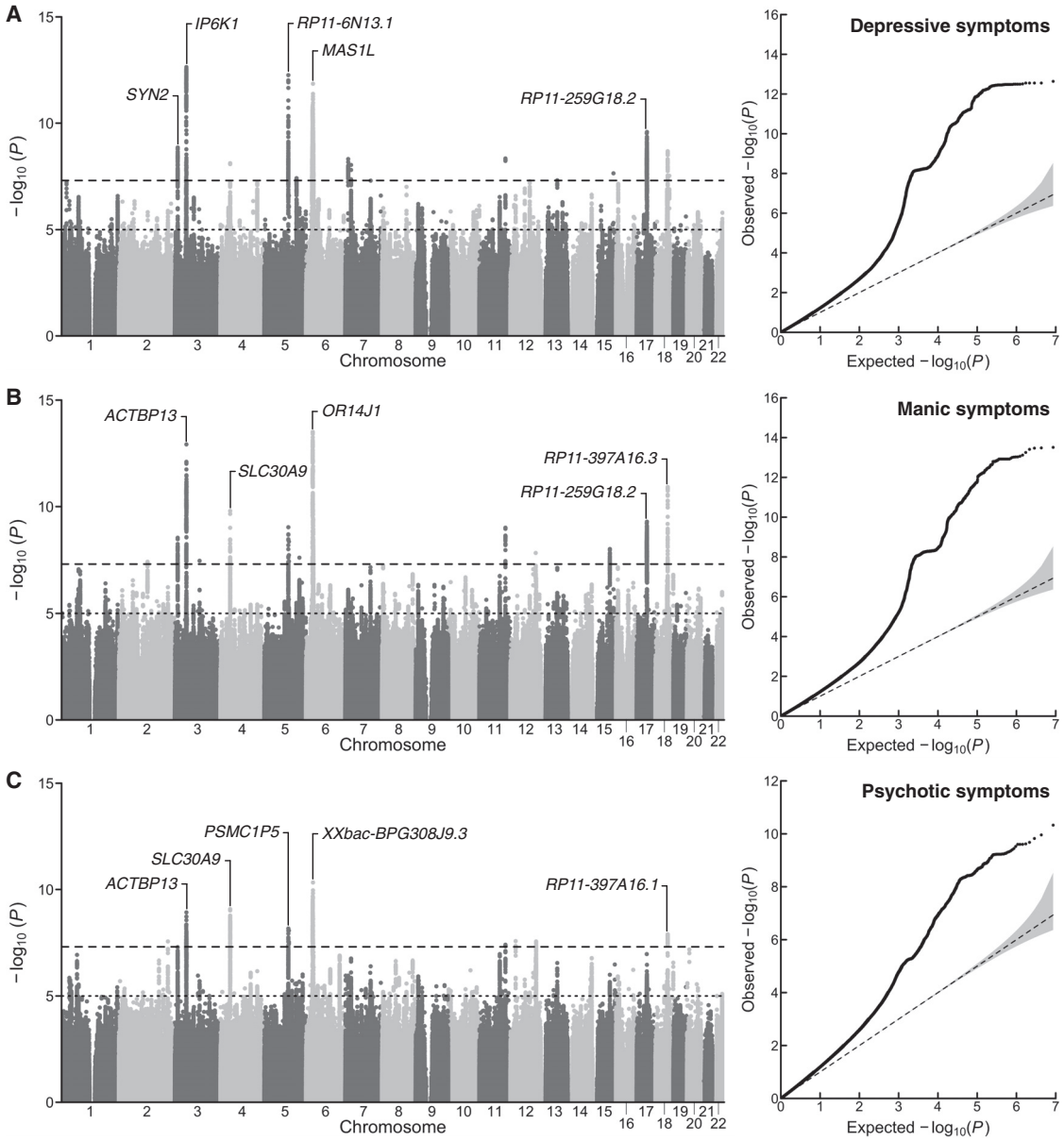

Figure 1. Univariate association results for lifetime measures of mood disturbance and psychosis

(A–C) Manhattan plots and a quantile-quantile plots for (A) depressive, (B) manic, and (C) psychotic symptoms. In the Manhattan plots, the x axis refers to chromosomal position, the y axis refers to the significance on a $-\log_{10}$ scale, the horizontal dashed line denotes genome-wide significance ($p = 5 \times 10^{-8}$), and the horizontal dotted line marks suggestive significance ($p = 5 \times 10^{-5}$). In the quantile-quantile plots, the x axis refers to expected p value, while the y axis refers to the observed p value. For each plot, the nearest gene for the lead SNP in the top five genome-wide significant loci is labeled.

and the second cluster comprised bipolar I, schizoaffective disorder, and schizophrenia. We then conducted an exploratory factor analysis (EFA) of the genetic covariance matrix, which produced results that were consistent with the groupings suggested by the hierarchical clustering algorithm. The correlated two-factor model with approximate simple structure suggested that phenotypes principally loaded onto one of two latent genetic factors with negligible cross-loadings (Figure 2B). Combined, these two correlated latent factors explained 81.3% of the total SNP-based genetic variances across phenotypes.

Finally, we formally modeled the genetic covariance matrix via confirmatory factor analysis (CFA). We based our model on the EFA results, which consisted of two correlated latent factors, F1 and F2. F1 can be conceptualized as capturing common psychopathology related to mood disturbance (including self-reported depressive, psychotic, and manic symptoms, as well as bipolar II and major depressive disorder), while F2 can be conceptualized as capturing rarer forms of serious mental illness (bipolar I, schizoaffective disorder, and schizophrenia). We did not estimate any cross-loadings. Instead, we estimated

Table 1. Summary of study phenotypes

GWAS (abbr.)	Source	N	h^2	λ_{GC}	Mean χ^2	Intercept	Ratio
Depressive symptoms (DEP)	present study	252,252	0.08	1.31	1.38	1.01	0.02
Manic symptoms (MAN)	present study	252,252	0.08	1.31	1.39	1.00	0.00
Psychotic symptoms (PSY)	present study	252,252	0.07	1.31	1.33	1.00	0.01
Major depressive D/O (MDD)	Wray et al., 2018[5]	138,884	0.10	1.19	1.20	1.00	<0
Bipolar II D/O (BD2)	Stahl et al., 2019[4]	25,576	0.10	1.07	1.08	1.03	0.42
Bipolar I D/O (BD1)	Stahl et al., 2019[4]	45,871	0.22	1.31	1.37	1.04	0.09
Schizoaffective D/O (SZA)	Stahl et al., 2019[4]	9,667	0.27	1.06	1.06	1.02	0.35
Schizophrenia (SCZ)	Ruderfer et al., 2018[21]	65,967	0.23	1.49	1.63	1.05	0.08
F1 (mood disturbance)	present study	377,518	N/A	1.44	1.53	1.05	0.10
F2 (serious mental illness)	present study	51,276	N/A	1.46	1.61	1.02	0.04

Heritability (h^2) was estimated using LD score regression. λ_{GC} refers to the median χ^2 statistic of the GWAS divided by the expected median of the χ^2 distribution with 1 degree of freedom. Mean χ^2 refers to the average χ^2 statistic of the GWAS. Intercept refers to the estimated intercept from univariate LD score regression. Ratio refers to a measure of stratification bias that is defined as (Intercept – 1)/(Mean χ^2 – 1). To harmonize measurement approaches among psychiatric disorders, summary statistics for MDD were obtained for the clinically ascertained cohorts, excluding 23andMe and UK Biobank. D/O, disorder; The effective sample size is reported for F1 and F2 (STAR Methods).

correlated residuals between bipolar I and bipolar II, as inspection of the genetic correlation matrix suggested a unique relationship between these disorders. The path diagram for this model is presented in Figure 2C.

We compared the correlated factor model with a common factor model, where all phenotypes were indicators of a single latent factor (i.e., a *p* factor) (Section 1.1 of supplemental methods; Figure S2). Briefly, we found that the common factor model showed suboptimal fit to the data, while the correlated factors model with correlated residuals for BD1 and BD2 showed excellent fit (Figure S3). Fit indices from the CFA indicated that the correlated factors model closely approximated the observed genetic covariance matrix ($\chi^2(18) = 496.16$, Akaike information criterion = 532.16, comparative fit index = 0.99, standardized root mean square residual = 0.06). That is, the patterns of covariance among the eight psychiatric phenotypes were most parsimoniously represented by two transdiagnostic latent factors at the genetic level, which were correlated only modestly ($r_g = 0.42$; SE = 0.03). This is a notable divergence from the factor structure frequently observed at the phenotypic level, including that seen with similar phenotypes in the UK Biobank (Section 1.1 of supplemental methods). However, we note that a direct comparison of phenotypic and genetic factor structure cannot be performed in the UK Biobank due to an insufficient number of clinical cases.

Transdiagnostic factors have markedly divergent genetic architectures

We then conducted a multivariate GWAS of the two latent genetic factors, F1 (N_{eff} = 377,518) and F2 (N_{eff} = 51,276). The results of these analyses are summarized in Table 1 and Figure 3. Briefly, we observed substantial inflation of the median test statistic for both F1 (λ_{GC} = 1.44, mean χ^2 = 1.53) and F2 (λ_{GC} = 1.46, mean χ^2 = 1.61), which is indicative of a robust polygenic signal for both factors (Figure S4). The LD score regression intercepts and attenuation ratios for F1 (intercept = 1.05, SE = 0.01; ratio = 0.10, SE = 0.02) and F2 (intercept = 1.02, SE = 0.01; ratio = 0.04, SE = 0.02) suggest that test-statistic inflation is primarily due to polygenic signal rather than bias.

After applying a standard clumping algorithm, we identified 26 and 59 independent loci associated with F1 and F2, respectively (Table 2; Tables S2A and S2B). Only five loci were associated with both factors. While many of these genomic regions have been previously identified in either the constituent GWASs or related studies, several contain novel discoveries. For example, several loci associated with F1 contain lead SNPs that have not been previously associated with psychopathology, such as rs13153844 ($p = 2.09 \times 10^{-9}$, nearest gene = *PSMC1P5*), rs1551765 ($p = 3.89 \times 10^{-8}$, nearest gene = *GRIA1*), rs147584788 ($p = 1.08 \times 10^{-8}$, nearest gene = AC003088.1), and rs8035987 ($p = 3.94 \times 10^{-8}$, nearest gene = *SIN3A*). Several loci associated with F2 also contain lead SNPs that were also novel risk variants for psychopathology, including rs2953329 ($p = 3.27 \times 10^{-8}$, nearest gene = *AKT3*), rs10199182 ($p = 1.56 \times 10^{-8}$, nearest gene = AC068490.2), rs9463650 ($p = 3.34 \times 10^{-8}$, nearest gene = *RPS17P5*), rs11603014 ($p = 2.32 \times 10^{-8}$, nearest gene = *RP11-890B15.2*), rs10777957 ($p = 1.79 \times 10^{-8}$, nearest gene = *ANKS1B*), and rs11064837 ($p = 2.43 \times 10^{-8}$, nearest gene = *RP11-768F21.1*).

Tests of heterogeneity suggested that the majority of observed SNP effects operate via the latent factors (i.e., associated SNPs primarily had consistent, pleiotropic effects on the constituent phenotypes). Indeed, Q_{SNP} tests identified no heterogeneous loci for F1 and only three heterogeneous loci for F2 with lead SNPs rs11696888 on chromosome 20 (Q_{SNP} $p = 2.04 \times 10^{-8}$; nearest gene = *STAU1*), rs1990042 on chromosome 7 (Q_{SNP} $p = 2.10 \times 10^{-8}$, nearest gene = AC004854.1), and rs3764002 on chromosome 12 (Q_{SNP} $p = 2.70 \times 10^{-8}$; nearest gene = *WSCD2*). Interestingly, the heterogeneous locus with lead SNP rs11696888 also contains rs200005157, which is a four base pair insertion/deletion that was previously identified as a locus with divergent effects on bipolar disorder and schizophrenia.21 Fine mapping conducted by Ruderfer and colleagues identified *CSE1L* as a plausible causal gene with divergent effects for bipolar disorder and schizophrenia on chromosome 20.

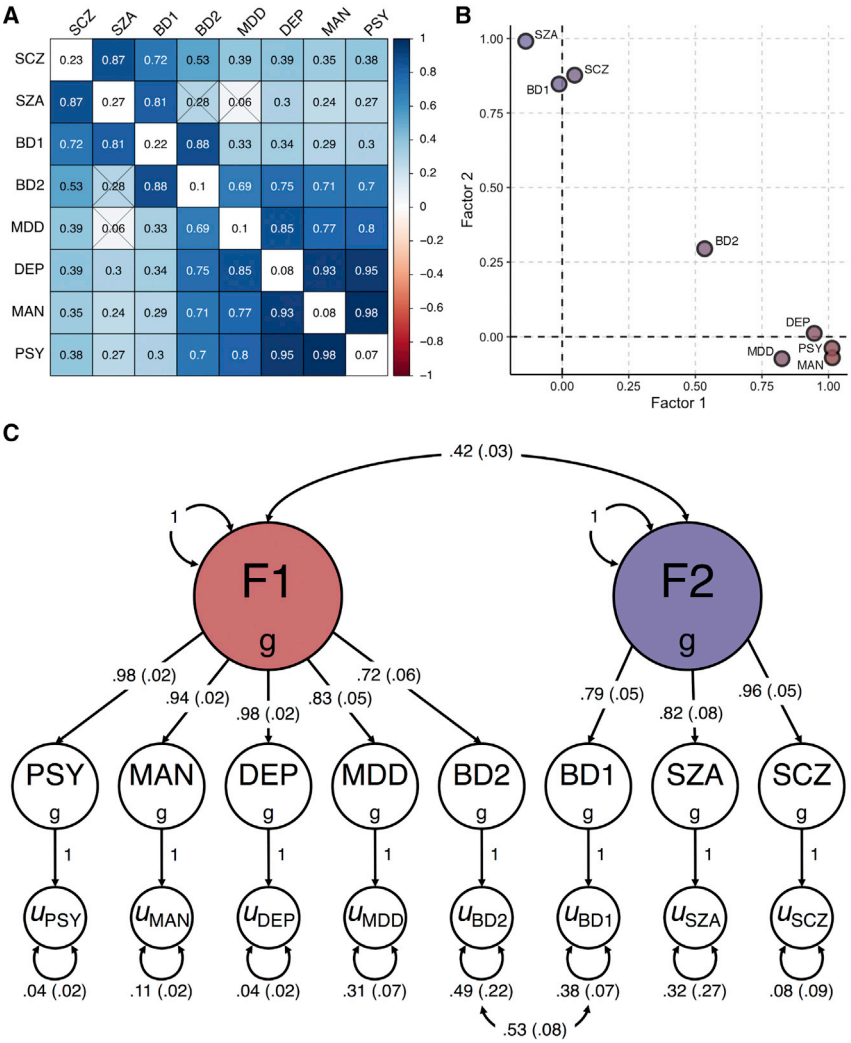

Figure 2. Relationships between eight psychiatric symptoms and disorders

(A) Matrix of bivariate genetic-correlation estimates, where the diagonal elements correspond to SNP h^2 and the off-diagonal elements correspond to genetic correlations. Estimates that are non-significant are crossed out.

(B) Scatterplot of standardized factor loadings from the exploratory factor analysis.

(C) Path diagram for the final confirmatory factor model with standardized parameter estimates.

Transdiagnostic factors are related to different aspects of neurobiology

To characterize the effects of variants associated with the transdiagnostic factors of psychopathology, we used FUMA to conduct a series of gene-mapping analyses. Specifically, we used positional mapping to align lead SNPs to genes based on genomic location, expression quantitative trait loci (eQTL) mapping to match *cis*-eQTL SNPs to genes whose expression they affect, and chromatin-interaction mapping to link SNPs to genes on the basis of three-dimensional DNA-DNA interactions. These three methods linked the associated SNPs for F1 and F2 to a combined 287 and 570 putative risk genes, respectively (Tables S2C–S2J). We then used MAGMA to conduct gene-based association analyses, which identified 115 and 243 genes associated with F1 and F2 (Tables S2K and S2L). Finally, we used S-Multi-Xcan to identify 50 and 91 genes associated with differential expression levels in brain tissue for F1 and F2, respectively (Tables S2M and S2N).

Collectively, these five approaches mapped a total of 332 genes to F1 and 710 genes to F2 (Figure 3). Only 159 of these putative risk genes were related to both factors. Focusing on genes implicated across all five methods, we found 11 genes robustly linked to F1 and 16 to F2 (Figure 3). Two genes (*PGBD1* and *XRCC3*) were related to both factors across all analyses. This limited overlap in mapped genes underscores the unique genetic architecture of each factor.

The modest genetic correlation between F1 and F2 ($r_g = 0.42$, SE = 0.03) implies that the majority of SNP-based genetic variance in each factor is unique from the other. To further characterize the shared and unique genetic architecture of these factors, we used HESS to estimate the local genetic covariance for 1,698 contiguous, similarly sized partitions across the genome. We found that approximately 27% of the genome explains 80% of the total genetic covariance between F1 and F2 and that only 15 genomic partitions share a significant local genetic correlation after correcting for multiple comparisons (Figure 4A).

Gene set enrichment and gene property (i.e., tissue expression) analyses further suggest that the genetic architectures of F1 and F2 are divergent at more granular levels of analysis, converging only at higher levels. While results from gene set enrichment analyses broadly implicated neurodevelopmental and neurobiological pathways for both factors, the specific molecular functions, cellular components, and biological processes tended to differ (Figure 4B; Tables S3A and S3B). For example, gene sets related to neurons were enriched for F1 and F2, but gene sets for specific parts of neurons were differentially enriched (e.g., the axon for F1 versus the somatodendritic compartment for F2). Similarly, in the tissue-expression analysis, we found that the brain was broadly implicated in the pathogenesis of psychopathology, as nearly all brain-related tissues were enriched for both F1 and F2 (Tables S3C and S3D). At the level of brain tissue, the only regions with divergent effects were the substantia nigra and brainstem, which were not significantly enriched for F1 after correction for multiple comparisons. However, shortcomings of these analyses include the relatively low spatial resolution of

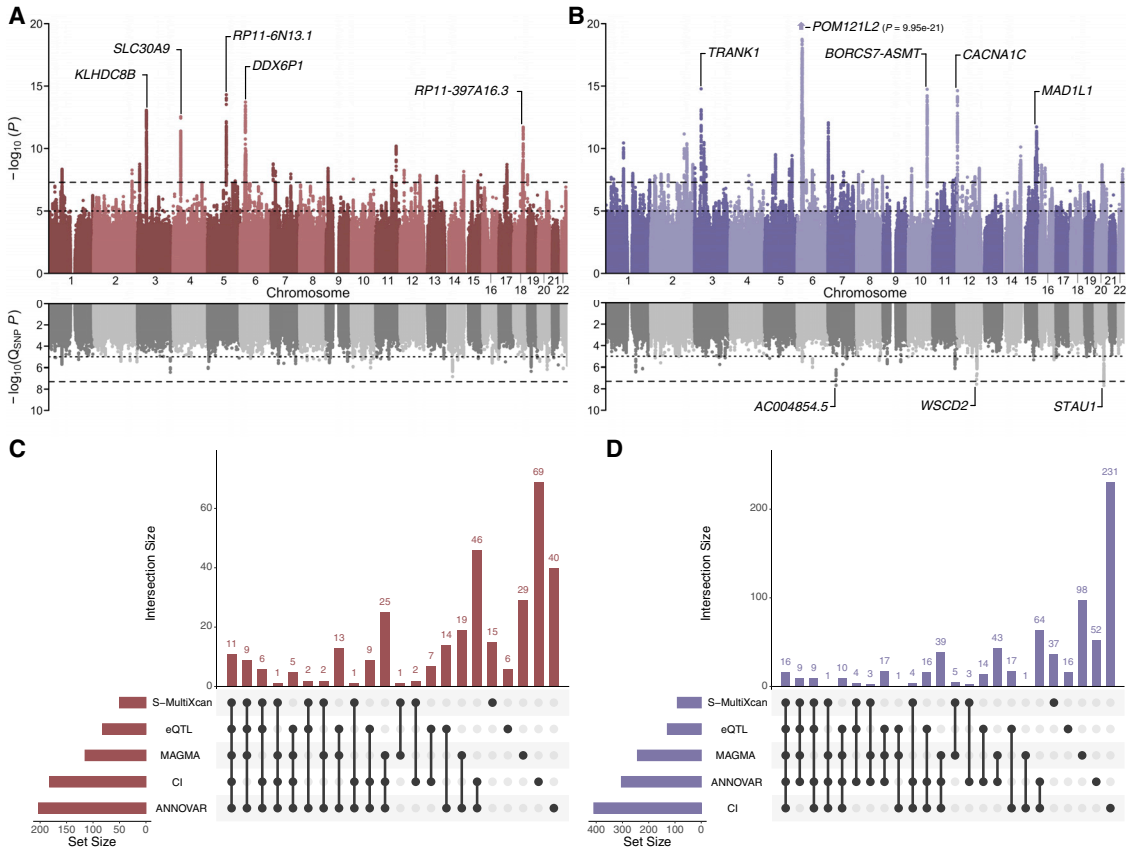

Figure 3. Multivariate association results for the two transdiagnostic latent genetic factors

(A and B) Miami plots for (A) F1 and (B) F2. The top of each Miami plot corresponds to the significance of SNP effects on each latent factor, as traditionally conveyed in a Manhattan plot, while the bottom corresponds to the significance of heterogeneity tests for SNP effects (Q_{SNP}; i.e., the degree to which SNP effects are not mediated by F1 or F2). For each plot, the x axis refers to chromosomal position, the y axis refers to the significance on a -$\log_{10}$ scale, the horizontal dashed line denotes genome-wide significance ($p = 5 \times 10^{-8}$), and the horizontal dotted line marks suggestive significance ($p = 5 \times 10^{-5}$). For each plot, the nearest gene for the lead SNP in the top five genome-wide significant loci is labeled.

(C and D) UpSet plots illustrating the intersection of the five gene-mapping methods, ranked by degree of overlap.

brain-related gene expression data and the limited sample size of the underlying data.

Therefore, to gain greater insight into potential etiological relationships between psychopathology and neurobiology, we estimated genetic correlations between the transdiagnostic factors of psychopathology and 101 morphological features of the human brain. Although we generally observed negative genetic correlations with cortical and subcortical features (i.e., greater risk for psychopathology was associated with smaller volumes across the brain) and positive with ventricular features (i.e., greater risk for psychopathology was associated with larger ventricular volumes), specific estimates between morphological features and F1 and F2 showed relatively little concordance (Figure 4C). After correcting for multiple comparisons, only the genetic correlation between F1 and the right middle temporal gyrus remained statistically significant ($r_g = -0.15$, SE = 0.04, $p = 3.98 \times 10^{-4}$) (Tables S3E and S3F).

We then used data from the Allen Human Brain Atlas to identify genes with transcriptomic profiles that were spatially similar to the neuroimaging genetic correlation maps for F1 and F2 (Tables S3G and S3H). Notably, these transcriptomically prioritized gene sets for F1 and F2 were entirely disjointed from one another and differentially expressed in pre-and postnatal cortical tissue from the PsychENCODE dataset (Figure 4D). We found that the developmental expression profile of the F1 gene set most closely resembled that of postnatal inhibitory neuronal genes, while the developmental expression profile of the F2 gene set most closely resembled that of prenatal inhibitory neuronal genes[25,26] (Figure S5). We note that the F1 and F2 gene sets also resemble postnatal microglia and prenatal neural progenitor cells, respectively, although to a lesser extent.

Transdiagnostic factors are differentially associated with human health and wellbeing

To better understand how these transdiagnostic genetic liabilities may manifest above and beyond their constituent phenotypes, we conducted a series of genetic correlation and polygenic prediction analyses focused on theoretically relevant phenotypes. In the genetic correlation analyses, we evaluated the relationships between the latent factors of psychopathology

Table 2. Lead SNPs for the top ten loci per latent factor from multivariate association analyses

Lead SNP	CHR:BP	A1	A2	MAF	*Z*	p	Nearest gene	Function	CADD	RDB
F1 (depressive symptoms, manic symptoms, psychotic symptoms, major depressive disorder, and bipolar II disorder)										
rs30266	5:103972357	G	A	0.32	−7.83	4.94×10^{-15}	*RP11-6N13.1*	ncRNA intronic	2.275	N/A
rs148682985	6:29288001	G	A	0.03	−7.66	1.93×10^{-14}	*DDX6P1*	intergenic	2.643	5
rs9586	3:49213637	C	T	0.02	7.46	8.80×10^{-14}	*KLHDC8B*	UTR3	11.63	N/A
rs28656217	4:42099424	T	C	0.16	7.30	2.85×10^{-13}	*SLC30A9*	intergenic	4.861	6
rs67526282	18:53471187	T	C	0.33	−7.04	1.97×10^{-12}	*RP11-397A16.3*	intergenic	7.656	6
rs7934649	11:113372671	C	T	0.36	−6.53	6.50×10^{-11}	*DRD2*	intergenic	1.426	7
rs17410557	18:50776391	T	C	0.38	−6.04	1.52×10^{-9}	*DCC*	intronic	4.502	7
rs3807866	7:12250378	G	A	0.40	−6.03	1.69×10^{-9}	*TMEM106B*	upstream	7.544	N/A
rs184262	3:12134740	A	G	0.15	6.02	1.77×10^{-9}	*SYN2*	ncRNA intronic	6.559	7
rs2696673	17:44315803	A	C	0.22	−6.01	1.89×10^{-9}	*RP11-259G18.2*	intergenic	3.3	N/A
F2 (bipolar I disorder, schizoaffective disorder, and schizophrenia)										
rs7746199	6:27261324	C	T	0.17	9.34	9.95×10^{-21}	*POM121L2*	intronic	0.879	1f
rs9834970	3:36856030	T	C	0.49	−7.96	1.67×10^{-15}	*TRANK1*	intergenic	11.17	4
rs12764899	10:104635103	G	A	0.23	7.95	1.82×10^{-15}	*C10orf32-ASMT:AS3MT*	intronic	1.133	7
rs4298967	12:2408194	A	G	0.34	7.92	2.37×10^{-15}	*CACNA1C*	intronic	10.73	5
rs6461049	7:2017445	C	T	0.44	−7.15	8.80×10^{-13}	*MAD1L1*	intronic	0.914	5
rs12902973	15:85105982	G	C	0.28	7.04	1.89×10^{-12}	*UBE2Q2P1*	ncRNA intronic	1.808	7
rs4380187	2:185811940	A	C	0.45	6.86	6.95×10^{-12}	*ZNF804A*	intergenic	2.923	7
rs2535627	3:52845105	T	C	0.50	6.63	3.36×10^{-11}	*ITIH4*	intergenic	5.307	N/A
rs1198588	1:98552832	A	T	0.23	−6.62	3.65×10^{-11}	*NFU1P2*	intergenic	1.829	3a
rs11693528	2:200736507	C	G	0.18	−6.60	4.18×10^{-11}	*AC073043.1*	ncRNA intronic	2.344	6

Results for all lead SNPs are presented in Tables S2A and S2B. Lead SNPs refer to approximately independent lead SNPs identified via FUMA. CHR:BP refers to genomic location of the lead SNP, specifically the chromosome and base pair location on that chromosome. A1 and A2 refer to the alleles for that SNP. MAF, minor allele frequency; CADD, Combined Annotation Dependent Depletion score; RDB, RegulomeDB score.

and 92 phenotypes broadly related to four broad domains of human health and wellbeing (Figure 5A; Table S4A). We found that genetic correlation estimates for F1 and F2 were moderately correlated across all broad domains (r = 0.60, p = 2.77×10^{-10}) as well as within each of the four domains: demography and socioeconomic status (r = 0.55, p = 1.17×10^{-2}), health and disease (r = 0.42, p = 1.17×10^{-2}), personality and risky behavior (r = 0.60, p = 3.05×10^{-3}), and psychopathology and cognition (r = 0.63, p = 1.57×10^{-2}). Generally, we found that F1 was more consistently correlated with phenotypes typically related to psychopathology than F2. This pattern was also observed in the partial genetic correlation analyses, where we found strong evidence of divergent genetic correlations after accounting for the overlap between F1 and F2 (Figure 5B; Table S4B). Indeed, partial genetic correlation estimates for F1 and F2 were negatively correlated across all domains (r = −0.43, p = 2.72×10^{-5}).

In the polygenic prediction analyses, we used electronic health records from the Vanderbilt University Medical Center biobank (BioVU) to evaluate the penetrance and pleiotropy of genetic risk for the transdiagnostic factors of psychopathology across 1,335 disease phenotypes, hereby referred to as "phecodes" (Figure 5C; Tables S4C and S4D). We found that polygenic scores for F1 and F2 were generally associated with all of the constituent phenotypes for both factors, but F1 was more strongly associated with mood-related phecodes, while F2 was more strongly associated with psychosis-related phecodes. Both polygenic scores for F1 and F2 shared associations with some forms of psychopathology (e.g., suicidality, posttraumatic stress disorder, substance-use disorders, and anxiety disorders) but diverged in their associations with others (e.g., personality disorders, paranoid disorders). Beyond psychopathology, F1 was more consistently associated a variety of medical phecodes, including those related to infectious diseases (e.g., viral hepatitis, HIV disease) and pervasive developmental disorders as well as diseases of the circulatory, digestive, endocrine, genitourinary, musculoskeletal, and respiratory systems.

DISCUSSION

By jointly analyzing genome-wide data for eight psychiatric disorders and symptoms in a novel multivariate framework, we identified two distinct transdiagnostic factors that distinguished common forms of psychopathology related to mood disturbance versus rare forms of serious mental illness. Together, these factors explained approximately 80% of the SNP-based genetic variance in mood and psychotic psychopathology but were themselves only moderately correlated. Extensive biological annotation of these two transdiagnostic factors revealed

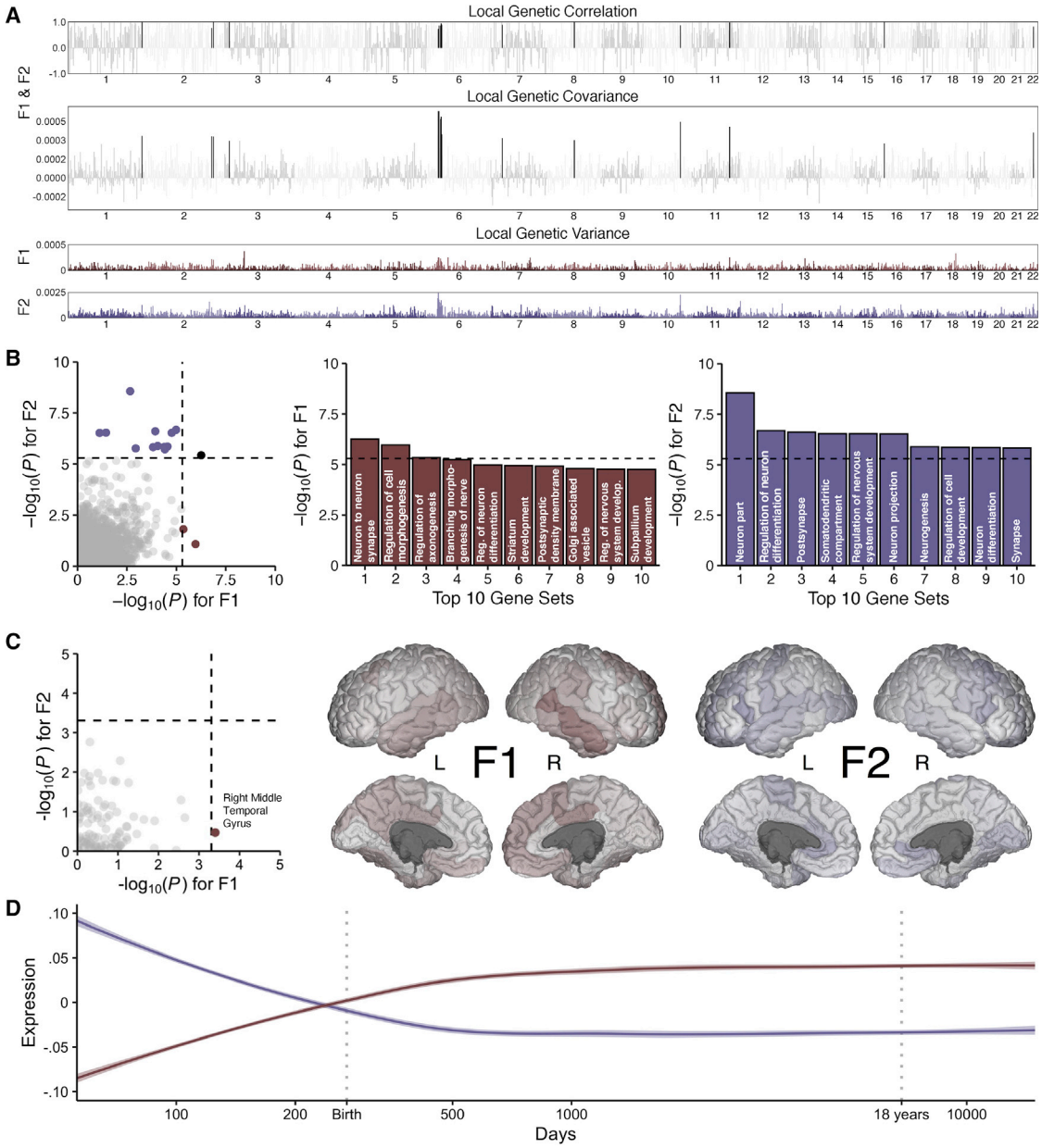

Figure 4. Biological annotation of the two transdiagnostic latent genetic factors

(A) Manhattan plots for local genetic correlation, covariance, and variance for F1 and F2. Black bars indicate significant local genetic correlation.

(B) Scatterplot of gene set enrichment results illustrating convergence and divergence across the latent genetic factors with accompanying histograms for the top 10 gene sets for each factor.

(C) Scatterplot of neuroimaging genetic-correlation results with accompanying figures where the $-\log_{10}$ p values are mapped across the cortex, as parcellated in the Desikan-Killiany-Tourville atlas.

(D) Smoothed line plots of gene set expression across developmental time in the PsychENCODE dataset for prioritized genes with transcriptomic profiles that are spatially similar to the neuroimaging genetic correlation maps for F1 and F2 (as indexed in the Allen Human Brain Atlas). For all plots, the dashed black line corresponds to the Bonferroni-corrected significance threshold when applicable.

clear differences between their factors in their underlying genetic architecture and biology. Further follow-up analyses highlighted additional differences between the factors in their associations with human wellbeing and disease. Our results provide four critical insights into the genetic architecture of forms of psychopathology characterized by mood disturbance and psychosis.

First, we built on genomic investigations of the dimensional structure of certain forms of psychopathology, such as a large-scale study of the mood-disorder spectrum,[27] and

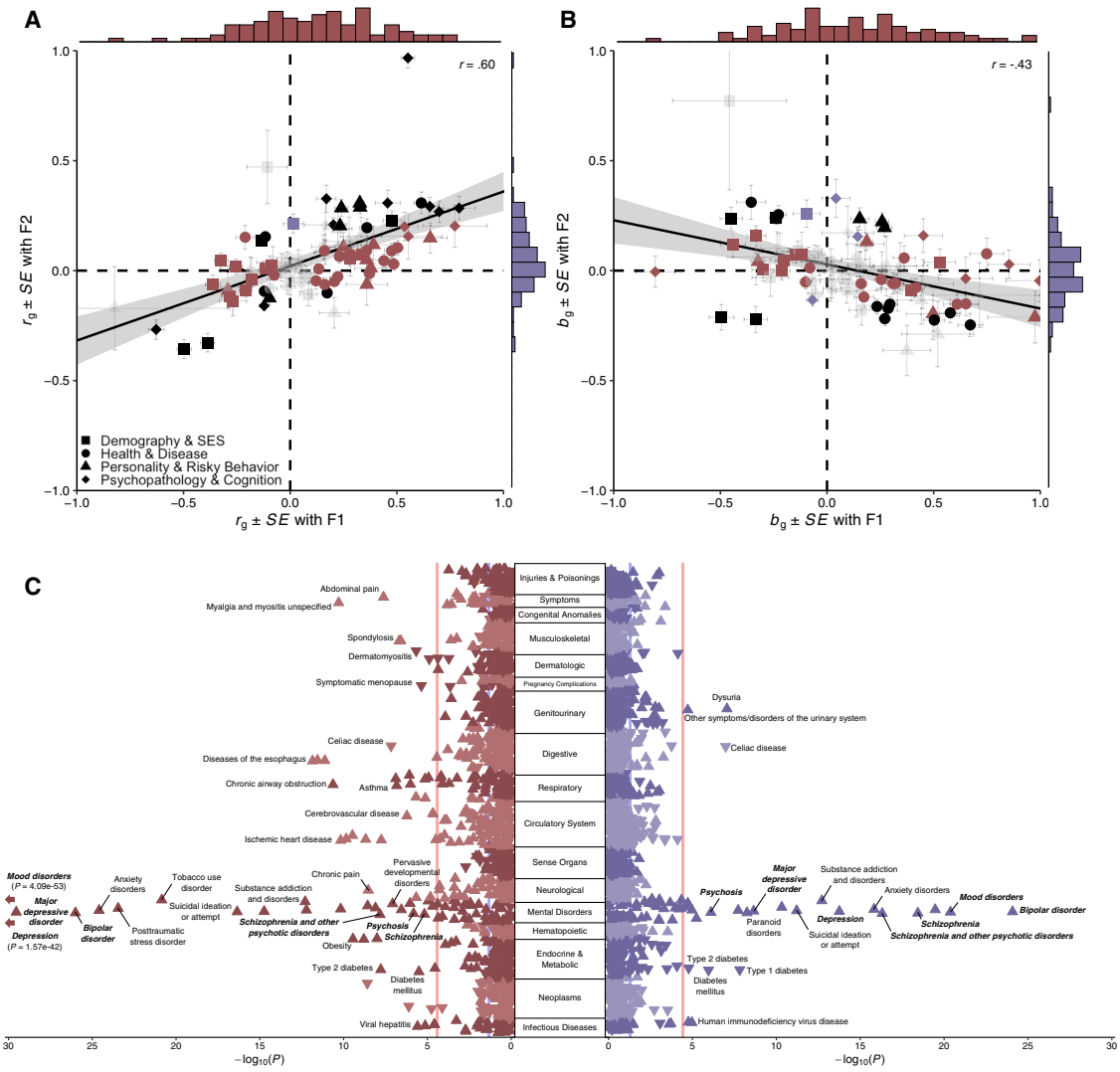

Figure 5. Genetic-correlation and phenome-wide association results for the two transdiagnostic latent genetic factors

(A) Scatterplot of genetic correlations (r_g) with marginal histograms.

(B) Scatterplot of partial genetic correlations (b_g) with marginal histograms. For both plots, phenotypes are grouped into one of four broad domains: (1) demography and socioeconomic status, (2) health and disease, (3) personality and risky behavior, and (4) psychopathology and cognition. A line of best fit (with 95% confidence interval) is fit for all 92 data points. Points are colored burgundy if significant only for F1, violet if significant only for F2, black if significant for both, and faded gray if non-significant for both. The standard errors (SEs) for point estimates are plotted for both factors.

(C) Rotated Miami plot for (left) F1 and (right) F2, where the y axis refers to the ICD-10 code category, the x axis refers to the significance on a $-\log_{10}$ scale, the vertical light red line denotes phenome-wide significance ($p = 3.27 \times 10^{-5}$) following Bonferroni correction, and the vertical light blue line marks nominal significance ($p = 0.05$). The direction of the triangle refers to the direction of effect. Phecodes closely resembling Genomic SEM model phenotypes are bolded and italicized for emphasis.

identified two transdiagnostic factors that explain the vast majority of SNP-based genetic variance in their constituent phenotypes. Perhaps surprisingly, variation in self-reported manic and psychotic symptoms is much more closely related to common forms of mood psychopathology (self-reported depressive symptoms, major depressive disorder, bipolar II disorder) than to psychiatric disorders characterized by severe mood disturbance and/or psychosis. These findings extend those of an earlier GWAS of psychotic experiences,[28] which also reported stronger genetic overlap with major depressive disorder than bipolar disorder or schizophrenia. Here, we also find that the factor structure at the genetic level is different than the factor structure that we observe at the phenotypic level in the UK Biobank with similar indicators. This finding contrasts with what has been called the ''phenotypic null hypothesis,'' which states that genetic and phenotypic factor structures are expected to converge.[29] Overall, these results illustrate how diagnostic boundaries, which are known to be problematic based on widespread phenotypic comorbidity, become even fuzzier at the genetic level of analysis.

Second, our multivariate association analyses identified 80 approximately independent loci associated with one of the transdiagnostic factors. Many of these genome-wide significant loci contain novel lead SNPs and map to genes that have not been previously associated with mood or psychotic psychopathology, such as *SIN3A*, which has been reported to be a key transcriptional regulator of cortical neurodevelopment, involved in neurogenesis and corticocortical projections in the developing mammalian brain.[30] Moreover, by employing multiple gene-mapping techniques, we were also able to triangulate on novel genes associated with psychopathology, including *WDR73*, the causal gene in a rare recessive autosomal disorder characterized by severe encephalopathy, developmental delay, and neurocognitive impairment.[31] Associations such as these are particularly interesting in light of results suggesting that genes disrupted in Mendelian disorders are also dysregulated by non-coding variants in phenotypically similar traits and disorders.[32] Furthermore, we build on the results of a large GWAS of eight psychiatric disorders[33] by providing novel evidence of factor-specific pleiotropy (i.e., consistent effects across a factor's constituent indicators) via Q_{SNP} results, which also identified several novel loci with significantly heterogeneous effects for bipolar I disorder, schizoaffective disorder, and schizophrenia.

Third, our extensive biological annotation revealed a marked divergence in the biology associated with the two transdiagnostic factors. While we find that the CNS is dually implicated at a broad systems-based level (e.g., non-specific enrichment of brain tissues), the biology associated with the two factors quickly diverges at more molecular levels of investigation. Via our novel approach to gene prioritization based on spatial transcriptomics, we identified two sets of factor-specific genes with contrasting developmental expression profiles. Specifically, we found that transcriptomically prioritized genes associated with the factor broadly characterized by common mood disturbance (F1) exhibited lower expression levels during early prenatal periods, while transcriptomically prioritized genes for the factor broadly characterized by rarer forms of serious mental illness (F2) exhibited higher expression levels during early prenatal periods. Notably, both of these trajectories identify the prenatal epoch as a critical developmental period related to psychopathology, albeit in different ways. These findings coalesce with and build upon previous studies that have begun to characterize developmental expression patterns of transdiagnostic genetic liabilities.[34] Here, we found that the two observed trajectories strongly resembled those of postnatal and prenatal inhibitory neuronal genes,[25] which have been implicated in the development of mood and psychotic disorders.[35–37]

Fourth, we found that the two factors differ substantially in their associations with human wellbeing and disease. Our results expand upon recent phenome-wide association studies of genetic risk for major depressive disorder[38] and schizophrenia,[39] expanding the list of complex traits and medical phenotypes associated with mood and psychotic psychopathology. We also identified an interesting pattern of results in our genetic correlation and phenome-wide association analyses, where the factor comprising more common forms of mood disturbance (F1) had broader and often stronger negative associations with socioeconomic and health-related outcomes than the factor comprising rarer forms of serious mental illness (F2). This runs counter to associations often observed at the phenotypic level, where individuals diagnosed with more serious mental illnesses tend to face more severe impairments and consequences in these domains.[40,41] These results raise questions about the potential ascertainment biases that affect GWASs. For example, clinically ascertained samples of people with diagnosed psychiatric disorders (particularly when those disorders are rare and seriously impairing) are subject to different sources of selection, attrition, and non-response than population-based studies that utilize self-report surveys. Consider, for instance, that individuals who are homeless and incarcerated in Western countries are drastically more likely than the general population to meet diagnostic criteria for a serious mental illness,[42,43] but these socially marginalized groups are less likely to have access to adequate mental health care or be included in medical research. This selective representation of psychopathology may induce collider bias and lead to misleading estimates of genetic association.[44] Indeed, cohort-level studies have already found that educational attainment polygenic scores are positively associated with research participation, while psychopathology polygenic scores are negatively associated.[45,46]

Limitations of the study

While we have taken many steps to address potential confounds, these major findings should be interpreted in light of several limitations. First, SEM does not reveal a "ground truth" about the nature of the phenotypes included in the analysis. Instead, it is a useful statistical framework for representing complex data structures, and latent factors are most appropriately considered as convenient statistical entities that explain the (co)variances of their indicators. As such, latent genetic factors are most useful as explanatory devices when accompanied by extensive biological annotation and follow up, as done in the present study. Second, the univariate GWASs are comprised of different samples with different measurement approaches and varying levels of power. However, we have made efforts to harmonize each of the GWASs used in Genomic SEM analyses (e.g., excluding self-rated measures from diagnostic phenotypes, and vice versa), and previous examination of these concerns suggest that the genetic factor structure is not biased by sample overlap or sample-size differences.[19,33]

Third, the univariate GWASs are comprised of different cohorts that may be subject to different sources of bias that cannot be fully quantified. For example, we note that the UK Biobank is subject to a volunteer selection bias, where study participants are generally healthier than individuals who are not study participants.[47] In ideal circumstances, the phenotypic and genetic factor analyses reported here would be performed within the same participants in order to minimize confounding by differences in sample selection. However, such deep phenotypic data are not currently available at the scale required for GWASs. Fourth, the current study focuses on forms of psychopathology that involve a wide variety of disturbances in mood and reality testing but does not comprehensively sample the full range of psychiatric disorders. These results thus complement other transdiagnostic research studies that have illuminated how schizophrenia

and bipolar I disorder diverge genetically from other clinically defined disorders, such as compulsive disorders and disorders of childhood.[33]

Conclusions

In summary, we have conducted a novel multivariate GWAS of multiple symptoms and disorders spanning mood and psychotic psychopathology. This analysis identified two transdiagnostic genetic liabilities operating quite distinctly from one another. Extensive biological annotation revealed contrasting genetic architectures that implicated prenatal neurodevelopment and neuronal function and regulation in markedly different ways. Given the degree of divergence between these two factors, future research is warranted to investigate the utility and appropriateness of even broader spectra of psychopathology (e.g., the *p* factor[20]) as explanatory devices at the level of molecular genetics. Collectively, our results suggest that the severity of mood and psychotic symptoms evident in severe psychiatric disorders might actually reflect a difference in kind rather than merely in degree.

STAR★METHODS

Detailed methods are provided in the online version of this paper and include the following:

- KEY RESOURCES TABLE
- RESOURCE AVAILABILITY
  - Lead contact
  - Materials availability
  - Data and code availability
- METHOD DETAILS
  - Phenotype construction in UK biobank
  - Univariate genome-wide association analyses
  - Multivariate genome-wide association analyses
  - Genetic correlations among study phenotypes
  - Exploratory factor analysis
  - Confirmatory factor analysis
  - Heritability for observed and latent phenotypes
  - Local heritability and genetic correlations
  - Gene mapping and identification
  - Gene-based association and enrichment analyses
  - Genetic correlation analyses between latent factors and other complex traits
  - Spatiotemporal transcriptomic analyses
  - Phenome-wide polygenic prediction

SUPPLEMENTAL INFORMATION

Supplemental information can be found online at https://doi.org/10.1016/j.xgen.2022.100140.

CONSORTIA

The members of the Bipolar Disorder Working Group of the Psychiatric Genomics Consortium are Eli A. Stahl, Gerome Breen, Andreas J. Forstner, Andrew McQuillin, Stephan Ripke, Vassily Trubetskoy, Manuel Mattheisen, Yunpeng Wang, Jonathan R.I. Coleman, Héléna A. Gaspar, Christiaan A. de Leeuw, Stacy Steinberg, Jennifer M. Whitehead Pavlides, Maciej Trzaskowski, Enda M. Byrne, Tune H. Pers, Peter A. Holmans, Alexander L. Richards, Liam Abbott, Esben Agerbo, Huda Akil, Diego Albani, Ney Alliey-Rodriguez, Thomas D. Als, Adebayo Anjorin, Verneri Antilla, Swapnil Awasthi, Judith A. Badner, Marie Bækvad-Hansen, Jack D. Barchas, Nicholas Bass, Michael Bauer, Richard Belliveau, Sarah E. Bergen, Carsten Bøcker Pedersen, Erlend Bøen, Marco P. Boks, James Boocock, Monika Budde, William Bunney, Margit Burmeister, Jonas Bybjerg-Grauholm, William Byerley, Miquel Casas, Felecia Cerrato, Pablo Cervantes, Kimberly Chambert, Alexander W. Charney, Danfeng Chen, Claire Churchhouse, Toni-Kim Clarke, William Coryell, David W. Craig, Cristiana Cruceanu, David Curtis, Piotr M. Czerski, Anders M. Dale, Simone de Jong, Franziska Degenhardt, Jurgen Del-Favero, J. Raymond DePaulo, Srdjan Djurovic, Amanda L. Dobbyn, Ashley Dumont, Torbjørn Elvsåshagen, Valentina Escott-Price, Chun Chieh Fan, Sascha B. Fischer, Matthew Flickinger, Tatiana M. Foroud, Liz Forty, Josef Frank, Christine Fraser, Nelson B. Freimer, Louise Frisén, Katrin Gade, Diane Gage, Julie Garnham, Claudia Giambartolomei, Marianne Giørtz Pedersen, Jaqueline Goldstein, Scott D. Gordon, Katherine Gordon-Smith, Elaine K. Green, Melissa J. Green, Tiffany A. Greenwood, Jakob Grove, Weihua Guan, José Guzman-Parra, Marian L. Hamshere, Martin Hautzinger, Urs Heilbronner, Stefan Herms, Maria Hipolito, Per Hoffmann, Dominic Holland, Laura Huckins, Stéphane Jamain, Jessica S. Johnson, Radhika Kandaswamy, Robert Karlsson, James L. Kennedy, Sarah Kittel-Schneider, James A. Knowles, Manolis Kogevinas, Anna C. Koller, Ralph Kupka, Catharina Lavebratt, Jacob Lawrence, William B. Lawson, Markus Leber, Phil H. Lee, Shawn E. Levy, Jun Z. Li, Chunyu Liu, Susanne Lucae, Anna Maaser, Donald J. MacIntyre, Pamela B. Mahon, Wolfgang Maier, Lina Martinsson, Steve McCarroll, Peter McGuffin, Melvin G. McInnis, James D. McKay, Helena Medeiros, Sarah E. Medland, Fan Meng, Lili Milani, Grant W. Montgomery, Derek W. Morris, Thomas W. Mühleisen, Niamh Mullins, Hoang Nguyen, Caroline M. Nievergelt, Annelie Nordin Adolfsson, Evaristus A. Nwulia, Claire O'Donovan, Loes M. Olde Loohuis, Anil P.S. Ori, Lilijana Oruc, Urban Ösby, Roy H. Perlis, Amy Perry, Andrea Pfennig, James B. Potash, Shaun M. Purcell, Eline J. Regeer, Andreas Reif, Céline S. Reinbold, John P. Rice, Fabio Rivas, Margarita Rivera, Panos Roussos, Douglas M. Ruderfer, Euijung Ryu, Cristina Sánchez-Mora, Alan F. Schatzberg, William A. Scheftner, Nicholas J. Schork, Cynthia Shannon Weickert, Tatyana Shehktman, Paul D. Shilling, Engilbert Sigurdsson, Claire Slaney, Olav B. Smeland, Janet L. Sobell, Christine Søholm Hansen, Anne T. Spijker, David St Clair, Michael Steffens, John S. Strauss, Fabian Streit, Jana Strohmaier, Szabolcs Szelinger, Robert C. Thompson, Thorgeir E. Thorgeirsson, Jens Treutlein, Helmut Vedder, Weiqing Wang, Stanley J. Watson, Thomas W. Weickert, Stephanie H. Witt, Simon Xi, Wei Xu, Allan H. Young, Peter Zandi, Peng Zhang, Sebastian Zöllner, Rolf Adolfsson, Ingrid Agartz, Martin Alda, Lena Backlund, Bernhard T. Baune, Frank Bellivier, Wade H. Berrettini, Joanna M. Biernacka, Douglas H.R. Blackwood, Michael Boehnke, Anders D. Børglum, Aiden Corvin, Nicholas Craddock, Mark J. Daly, Udo Dannlowski, Tõnu Esko, Bruno Etain, Mark Frye, Janice M. Fullerton, Elliot S. Gershon, Michael Gill, Fernando Goes, Maria Grigoroiu-Serbanescu, Joanna Hauser, David M. Hougaard, Christina M. Hultman, Ian Jones, Lisa A. Jones, René S. Kahn, George Kirov, Mikael Landén, Marion Leboyer, Cathryn M. Lewis, Qingqin S. Li, Jolanta Lissowska, Nicholas G. Martin, Fermin Mayoral, Susan L. McElroy, Andrew M. McIntosh, Francis J. McMahon, Ingrid Melle, Andres Metspalu, Philip B. Mitchell, Gunnar Morken, Ole Mors, Preben Bo Mortensen, Bertram Müller-Myhsok, Richard M. Myers, Benjamin M. Neale, Vishwajit Nimgaonkar, Merete Nordentoft, Markus M. Nöthen, Michael C. O'Donovan, Ketil J. Oedegaard, Michael J. Owen, Sara A. Paciga, Carlos Pato, Michele T. Pato, Danielle Posthuma, Josep Antoni Ramos-Quiroga, Marta Ribasés, Marcella Rietschel, Guy A. Rouleau, Martin Schalling, Peter R. Schofield, Thomas G. Schulze, Alessandro Serretti, Jordan W. Smoller, Hreinn Stefansson, Kari Stefansson, Eystein Stordal, Patrick F. Sullivan, Gustavo Turecki, Arne E. Vaaler, Eduard Vieta, John B. Vincent, Thomas Werge, John I. Nurnberger, Naomi R. Wray, Arianna Di Florio, Howard J. Edenberg, Sven Cichon, Roel A. Ophoff, Laura J. Scott, Ole A. Andreassen, John Kelsoe, and Pamela Sklar. Their affiliations are provided in the supplemental information.

ACKNOWLEDGMENTS

T.T.M. is supported by funds from NIH T32HG010464. S.S.-R. was supported by funds from the California Tobacco-Related Disease Research Program

(TRDRP; grant number T29KT0526) and NIDA DP1DA054394. J.S. was supported by NIH T32MH019112. A.O. was supported by the Netherlands Organisation for Scientific Research VENI (016.Veni.198.058). A.A.P. was supported by a grant from the TRDRP (28IR-0070) and by NIH P50DA037844. K.P.H. and E.M.T.-D. were supported in part by Jacobs Foundation Research Fellowships and are faculty research associates of the Population Research Center at the University of Texas at Austin, which is supported by NIH grant P2CHD04284. K.P.H. and E.M.T.-D. were also supported by NIH grants R01-HD083613 and R01-HD092548. E.M.T.-D. was also supported by NIH grant R01-MH120219and is a member of the Center for Aging and Population Studies at the University of Texas at Austin, which is supported by NIH grant P30AG066614. M.C.K. was supported by funds from NIH grants MH100141 and DA044283. P.D.K. was supported by an ERC consolidator grant (647648 EdGe). The dataset(s) used for the PheWAS/LabWAS analyses described were obtained from Vanderbilt University Medical Center's BioVU, which is supported by numerous sources: institutional funding, private agencies, and federal grants. These include the NIH-funded Shared Instrumentation Grant S10RR025141 and CTSA grants UL1TR002243, UL1TR000445, and UL1RR024975. Genomic data are also supported by investigator-led projects that include U01HG004798, R01NS032830, RC2GM092618, P50GM115305, U01HG006378, U19HL065962, and R01HD074711, and additional funding sources are listed at https://victr.vumc.org/biovu-funding/. L.K.D. obtained support from 1R01MH113362, 1R01MH118233, and 1R56MH120736. The project was approved by the VUMC Institutional Review Board (IRB #160302, #172020, and #190418). Its contents are solely the responsibility of the authors and do not necessarily represent official views of the National Center for Advancing Translational Sciences or the National Institutes of Health. This research was conducted with the UK Biobank Resource under application number 11425 and with the support and collaboration from all investigators who make up the Bipolar Disorder Working Group of the PGC. We would like to thank the many studies that made these consortia possible, the researchers involved, and the participants in those studies, without whom this effort would not be possible. We would also like to thank the research participants and employees of 23andMe for making this work possible.

AUTHOR CONTRIBUTIONS

T.T.M., P.D.K., and K.P.H. conceived and designed the study. P.D.K. and K.P.H. oversaw the study. T.T.M. and K.P.H. led the writing of the manuscript with substantive contributions from P.D.K. and M.C.K. A.A.P., E.M.T.-D., and K.S.K. provided valuable feedback on the framing and interpretation of the results. T.T.M. was the lead analyst, responsible for conducting GWASs, quality control, genetic correlations, multivariate analyses with Genomic SEM, and biological annotation with assistance from R.K.L., A.D.G., S.S.-R., and J.S. T.T.M. prepared the data for analysis with assistance from R.K.L., A.O., R.d.V., and S.F.W.M. S.S.-R. performed the phenome-wide association study with assistance from L.K.D. T.T.M. prepared the figures and tables. Investigators from the Bipolar Disorder Working Group of the PGC contributed data for BD1, BD2, and SZA. All authors provided valuable feedback and advice during preparation of the manuscript.

DECLARATION OF INTERESTS

The authors declare no competing interests.

Received: November 13, 2020
Revised: October 25, 2021
Accepted: May 10, 2022
Published: June 8, 2022

REFERENCES

1. Vos, T., Abajobir, A.A., Abate, K.H., Abbafati, C., Abbas, K.M., Abd-Allah, F., Abdulkader, R.S., Abdulle, A.M., Abebo, T.A., Abera, S.F., et al. (2017). Global, regional, and national incidence, prevalence, and years lived with disability for 328 diseases and injuries for 195 countries, 1990–2016: a systematic analysis for the Global Burden of Disease Study 2016. Lancet *390*, 1211–1259.
2. Polderman, T.J.C., Benyamin, B., de Leeuw, C.A., Sullivan, P.F., van Bochoven, A., Visscher, P.M., and Posthuma, D. (2015). Meta-analysis of the heritability of human traits based on fifty years of twin studies. Nat. Genet. *47*, 702–709. advance on.
3. Ripke, S., Neale, B.M., Corvin, A., Walters, J.T.R., Farh, K.-H., Holmans, P.A., Lee, P., Bulik-Sullivan, B., Collier, D.A., Huang, H., et al. (2014). Biological insights from 108 schizophrenia-associated genetic loci. Nature *511*, 421–427.
4. Stahl, E.A., Breen, G., Forstner, A.J., McQuillin, A., Ripke, S., Trubetskoy, V., Mattheisen, M., Wang, Y., Coleman, J.R.I., Gaspar, H.A., et al. (2019). Genome-wide association study identifies 30 loci associated with bipolar disorder. Nat. Genet. *51*, 793–803.
5. Wray, N.R., Ripke, S., Mattheisen, M., Trzaskowski, M., Byrne, E.M., Abdellaoui, A., Adams, M.J., Agerbo, E., Air, T.M., Andlauer, T.M.F., et al. (2018). Genome-wide association analyses identify 44 risk variants and refine the genetic architecture of major depression. Nat. Genet. *50*, 668–681.
6. Anttila, V., Bulik-Sullivan, B., Finucane, H.K., Walters, R.K., Bras, J., Duncan, L., Escott-Price, V., Falcone, G.J., Gormley, P., Malik, R., et al. (2018). Analysis of shared heritability in common disorders of the brain. Science *360*, eaap8757.
7. Lee, J.J., Wedow, R., Okbay, A., Kong, E., Maghzian, O., Zacher, M., Nguyen-Viet, T.A., Bowers, P., Sidorenko, J., Linnér, R.K., et al. (2018). Gene discovery and polygenic prediction from a 1.1-million-person GWAS of educational attainment. Nat. Genet. *50*, 1112.
8. O'Donovan, M.C., and Owen, M.J. (2016). The implications of the shared genetics of psychiatric disorders. Nat. Med. *22*, 1214.
9. Insel, T., Cuthbert, B., Garvey, M., Heinssen, R., Pine, D.S., Quinn, K., Sanislow, C., and Wang, P. (2010). Research Domain Criteria (RDoC): Toward a New Classification Framework for Research on Mental Disorders.
10. Cuthbert, B.N. (2014). The RDoC framework: facilitating transition from ICD/DSM to dimensional approaches that integrate neuroscience and psychopathology. World Psychiatry *13*, 28–35.
11. Howard, D.M., Adams, M.J., Clarke, T.-K., Hafferty, J.D., Gibson, J., Shirali, M., Coleman, J.R.I., Hagenaars, S.P., Ward, J., Wigmore, E.M., et al. (2019). Genome-wide meta-analysis of depression identifies 102 independent variants and highlights the importance of the prefrontal brain regions. Nat. Neurosci. *22*, 343.
12. Sanchez-Roige, S., Palmer, A.A., Fontanillas, P., Elson, S.L., 23andMe Research Team, the S.U.D.W.G. of the P.G.C.; Adams, M.J., Howard, D.M., Edenberg, H.J., Davies, G., Crist, R.C., et al. (2018). Genome-wide association study meta-analysis of the alcohol use disorders identification test (AUDIT) in two population-based cohorts. Am. J. Psychiatry *176*, 107–118.
13. Levey, D.F., Gelernter, J., Polimanti, R., Zhou, H., Cheng, Z., Aslan, M., Quaden, R., Concato, J., Radhakrishnan, K., Bryois, J., et al. (2020). Reproducible genetic risk loci for anxiety: results From∼ 200,000 participants in the million veteran Program. Am. J. Psychiatry, appi–ajp. https://doi.org/10.1176/appi.ajp.2019.19030256.
14. Bycroft, C., Freeman, C., Petkova, D., Band, G., Elliott, L.T., Sharp, K., Motyer, A., Vukcevic, D., Delaneau, O., O'Connell, J., et al. (2018). The UK Biobank resource with deep phenotyping and genomic data. Nature *562*, 203–209.
15. Sanchez-Roige, S., and Palmer, A.A. (2020). Emerging phenotyping strategies will advance our understanding of psychiatric genetics. Nat. Neurosci. *23*, 475–480. https://doi.org/10.1038/s41593-020-0609-7.
16. Plomin, R., Haworth, C.M.A., and Davis, O.S.P. (2009). Common disorders are quantitative traits. Nat. Rev. Genet. *10*, 872–878. https://doi.org/10.1038/nrg2670.

17. van den Berg, S.M., Glas, C.A.W., and Boomsma, D.I. (2007). Variance decomposition using an IRT measurement model. Behav. Genet. *37*, 604–616. https://doi.org/10.1007/s10519-007-9156-1.

18. Cheesman, R., Purves, K.L., Pingault, J.-B., Breen, G., Plomin, R., Rijsdij K, F., Eley, T.C., and others. (2018). Extracting stability increases the SNP heritability of emotional problems in young people. Transl. Psychiatry *8*, 223–229. https://doi.org/10.1038/s41398-018-0269-5.

19. Grotzinger, A.D., Rhemtulla, M., de Vlaming, R., Ritchie, S.J., Mallard, T.T., Hill, W.D., Ip, H.F., Marioni, R.E., McIntosh, A.M., Deary, I.J., et al. (2019). Genomic structural equation modelling provides insights into the multivariate genetic architecture of complex traits. Nat. Hum. Behav. *3*, 513–525. https://doi.org/10.1038/s41562-019-0566-x.

20. Caspi, A., Houts, R.M., Belsky, D.W., Goldman-Mellor, S.J., Harrington, H., Israel, S., Meier, M.H., Ramrakha, S., Shalev, I., Poulton, R., and Moffitt, T.E. (2014). The p factor: one general psychopathology factor in the structure of psychiatric disorders? Clin. Psychol. Sci. *2*, 119–137. https://doi.org/10.1177/2167702613497473.

21. Ruderfer, D.M., Ripke, S., McQuillin, A., Boocock, J., Stahl, E.A., Pavlides, J.M.W., Mullins, N., Charney, A.W., Ori, A.P.S., Loohuis, L.M.O., et al. (2018). Genomic dissection of bipolar disorder and schizophrenia, including 28 subphenotypes. Cell *173*, 1705–1715. https://doi.org/10.1016/j.cell.2018.05.046.

22. Okbay, A., Baselmans, B.M.L., De Neve, J.-E., Turley, P., Nivard, M.G., Fontana, M.A., Meddens, S.F.W., Linnér, R.K., Rietveld, C.A., Derringer, J., et al. (2016). Genetic variants associated with subjective well-being, depressive symptoms, and neuroticism identified through genome-wide analyses. Nat. Genet. *48*, 624–633. https://doi.org/10.1038/ng.3552.

23. Nagel, M., Jansen, P.R., Stringer, S., Watanabe, K., de Leeuw, C.A., Bryois, J., Savage, J.E., Hammerschlag, A.R., Skene, N.G., Muñoz-Manchado, A.B., et al. (2018). Meta-analysis of genome-wide association studies for neuroticism in 449,484 individuals identifies novel genetic loci and pathways. Nat. Genet. *50*, 920–927. https://doi.org/10.1038/s41588-018-0151-7.

24. Pardiñas, A.F., Holmans, P., Pocklington, A.J., Escott-Price, V., Ripke, S., Carrera, N., Legge, S.E., Bishop, S., Cameron, D., Hamshere, M.L., et al. (2018). Common schizophrenia alleles are enriched in mutation-intolerant genes and in regions under strong background selection. Nat. Genet. *50*, 381–389. https://doi.org/10.1038/s41588-018-0059-2.

25. Lake, B.B., Chen, S., Sos, B.C., Fan, J., Kaeser, G.E., Yung, Y.C., Duong, T.E., Gao, D., Chun, J., Kharchenko, P.V., and Zhang, K. (2018). Integrative single-cell analysis of transcriptional and epigenetic states in the human adult brain. Nat. Biotechnol. *36*, 70–80. https://doi.org/10.1038/nbt.4038.

26. Li, M., Santpere, G., Imamura Kawasawa, Y., Evgrafov, O.V., Gulden, F.O., Pochareddy, S., Sunkin, S.M., Li, Z., Shin, Y., Zhu, Y., et al. (2018). Integrative functional genomic analysis of human brain development and neuropsychiatric risks. Science *362*, eaat7615. https://doi.org/10.1126/science.aat7615.

27. Coleman, J.R.I., Gaspar, H.A., Bryois, J., Byrne, E.M., Forstner, A.J., Holmans, P.A., de Leeuw, C.A., Mattheisen, M., McQuillin, A., Pavlides, J.M.W., et al. (2019). The genetics of the mood disorder spectrum: genome-wide association analyses of more than 185,000 cases and 439,000 controls. Biol. Psychiatry *88*, 169–184.

28. Legge, S.E., Jones, H.J., Kendall, K.M., Pardiñas, A.F., Menzies, G., Bracher-Smith, M., Escott-Price, V., Rees, E., Davis, K.A.S., Hotopf, M., et al. (2019). Association of genetic liability to psychotic experiences with neuropsychotic disorders and traits. JAMA Psychiatry *76*, 1256–1265. https://doi.org/10.1001/jamapsychiatry.2019.2508.

29. Turkheimer, E., Pettersson, E., and Horn, E.E. (2014). A phenotypic null hypothesis for the genetics of personality. Annu. Rev. Psychol. *65*, 515–540. https://doi.org/10.1146/annurev-psych-113011-143752.

30. Witteveen, J.S., Willemsen, M.H., Dombroski, T.C.D., Van Bakel, N.H.M., Nillesen, W.M., Van Hulten, J.A., Jansen, E.J.R., Verkaik, D., Veenstra-Knol, H.E., van Ravenswaaij-Arts, C.M.A., et al. (2016). Haploinsufficiency of MeCP2-interacting transcriptional co-repressor SIN3A causes mild intellectual disability by affecting the development of cortical integrity. Nat. Genet. *48*, 877–887. https://doi.org/10.1038/ng.3619.

31. Colin, E., Huynh Cong, E., Mollet, G., Guichet, A., Gribouval, O., Arrondel, C., Boyer, O., Daniel, L., Gubler, M.-C., Ekinci, Z., et al. (2014). Loss-of-function mutations in WDR73 are responsible for microcephaly and steroid-resistant nephrotic syndrome: galloway-Mowat syndrome. Am. J. Hum. Genet. *95*, 637–648. https://doi.org/10.1016/j.ajhg.2014.10.011.

32. Freund, M.K., Burch, K.S., Shi, H., Mancuso, N., Kichaev, G., Garske, K.M., Pan, D.Z., Miao, Z., Mohlke, K.L., Laakso, M., et al. (2018). Phenotype-specific enrichment of Mendelian disorder genes near GWAS regions across 62 complex traits. Am. J. Hum. Genet. *103*, 535–552. https://doi.org/10.1016/j.ajhg.2018.08.017.

33. Lee, P.H., Anttila, V., Won, H., Feng, Y.-C.A., Rosenthal, J., Zhu, Z., Tucker-Drob, E.M., Nivard, M.G., Grotzinger, A.D., Posthuma, D., et al. (2019). Genomic relationships, novel loci, and pleiotropic mechanisms across eight psychiatric disorders. Cell *179*, 1469–1482.

34. Schork, A.J., Won, H., Appadurai, V., Nudel, R., Gandal, M., Delaneau, O., Revsbech Christiansen, M., Hougaard, D.M., Bækved-Hansen, M., Bybjerg-Grauholm, J., et al. (2019). A genome-wide association study of shared risk across psychiatric disorders implicates gene regulation during fetal neurodevelopment. Nat. Neurosci. *22*, 353–361. https://doi.org/10.1038/s41593-018-0320-0.

35. Volk, D.W., and Lewis, D.A. (2014). Early developmental disturbances of cortical inhibitory neurons: contribution to cognitive deficits in schizophrenia. Schizophr. Bull. *40*, 952–957. https://doi.org/10.1093/schbul/sbu111.

36. Fine, R., Zhang, J., and Stevens, H.E. (2014). Prenatal stress and inhibitory neuron systems: implications for neuropsychiatric disorders. Mol. Psychiatry *19*, 641–651. https://doi.org/10.1038/mp.2014.35.

37. Duman, R.S., Sanacora, G., and Krystal, J.H. (2019). Altered connectivity in depression: GABA and glutamate neurotransmitter deficits and reversal by novel treatments. Neuron *102*, 75–90. https://doi.org/10.1016/j.neuron.2019.03.013.

38. Dennis, J., Sealock, J., Levinson, R.T., Farber-Eger, E., Franco, J., Fong, S., Straub, P., Hucks, D., Linton, M.F., Song, W.-L., et al. (2019). Genetic risk for major depressive disorder and loneliness in gender-specific associations with coronary artery disease. Preprint at bioRxiv, 512541. https://doi.org/10.1038/s41380-019-0614-y.

39. Zheutlin, A.B., Dennis, J., Karlsson Linnér, R., Moscati, A., Restrepo, N., Straub, P., Ruderfer, D., Castro, V.M., Chen, C.-Y., Ge, T., et al. (2019). Penetrance and pleiotropy of polygenic risk scores for schizophrenia in 106,160 patients across four health care systems. Am. J. Psychiatry *176*, 846–855. https://doi.org/10.1176/appi.ajp.2019.18091085.

40. Lewis, D.A., and Levitt, P. (2002). Schizophrenia as a disorder of neurodevelopment. Annu. Rev. Neurosci. *25*, 409–432. https://doi.org/10.1146/annurev.neuro.25.112701.142754.

41. Laursen, T.M., Nordentoft, M., and Mortensen, P.B. (2014). Excess early mortality in schizophrenia. Annu. Rev. Clin. Psychol. *10*, 425–448. https://doi.org/10.1146/annurev-clinpsy-032813-153657.

42. Fazel, S., and Danesh, J. (2002). Serious mental disorder in 23 000 prisoners: a systematic review of 62 surveys. Lancet *359*, 545–550. https://doi.org/10.1016/S0140-6736(02)07740-1.

43. Fazel, S., Geddes, J.R., and Kushel, M. (2014). The health of homeless people in high-income countries: descriptive epidemiology, health consequences, and clinical and policy recommendations. Lancet *384*, 1529–1540. https://doi.org/10.1016/S0140-6736(14)61132-6.

44. Munafò, M.R., Tilling, K., Taylor, A.E., Evans, D.M., and Davey Smith, G. (2018). Collider scope: when selection bias can substantially influence observed associations. Int. J. Epidemiol. *47*, 226–235. https://doi.org/10.1093/ije/dyx206.

45. Martin, J., Tilling, K., Hubbard, L., Stergiakouli, E., Thapar, A., Davey Smith, G., O'Donovan, M.C., and Zammit, S. (2016). Association of genetic risk for schizophrenia with nonparticipation over time in a

population-based cohort study. Am. J. Epidemiol. *183*, 1149–1158. https://doi.org/10.1093/aje/kww009.

46. Taylor, A.E., Jones, H.J., Sallis, H., Smith, G.D., Lawlor, D., Davies, N.M., Zammit, S., Lawlor, D.A., Munafò, M.R., Davey Smith, G., et al. (2018). Exploring the association of genetic factors with participation in the avon longitudinal study of parents and children. Int. J. Epidemiol. *47*, 1207–1216. https://doi.org/10.1093/ije/dyy060.
47. Fry, A., Littlejohns, T.J., Sudlow, C., Doherty, N., Adamska, L., Sprosen, T., Collins, R., and Allen, N.E. (2017). Comparison of sociodemographic and health-related characteristics of UK biobank participants with those of the general population. Am. J. Epidemiol. *186*, 1026–1034. https://doi.org/10.1093/aje/kwx246.
48. Muthén, L.K., and Muthén, B. (2016). Mplus. The Comprehensive Modelling Program for Applied Researchers: User's Guide.
49. Loh, P.-R., Tucker, G., Bulik-Sullivan, B.K., Vilhjálmsson, B.J., Finucane, H.K., Salem, R.M., Chasman, D.I., Ridker, P.M., Neale, B.M., Berger, B., et al. (2015). Efficient Bayesian mixed-model analysis increases association power in large cohorts. Nat. Genet. *47*, 284–290. https://doi.org/10.1038/ng.3190.
50. Abraham, G., Qiu, Y., and Inouye, M. (2017). FlashPCA2: principal component analysis of Biobank-scale genotype datasets. Bioinformatics.
51. Winkler, T.W., Day, F.R., Croteau-Chonka, D.C., Wood, A.R., Locke, A.E., Mägi, R., Ferreira, T., Fall, T., Graff, M., Justice, A.E., et al. (2014). Quality control and conduct of genome-wide association meta-analyses. Nat. Protoc. *9*, 1192–1212. https://doi.org/10.1038/nprot.2014.071.
52. Bulik-Sullivan, B.K., Finucane, H.K., Anttila, V., Gusev, A., Day, F.R., Loh, P.-R., Duncan, L., Perry, J.R.B., Patterson, N., Robinson, E.B., et al. (2015). An atlas of genetic correlations across human diseases and traits. Nat. Genet. *47*, 1236–1241. https://doi.org/10.1038/ng.3406.
53. Shi, H., Kichaev, G., and Pasaniuc, B. (2016). Contrasting the genetic architecture of 30 complex traits from summary association data. Am. J. Hum. Genet. *99*, 139–153.
54. Shi, H., Mancuso, N., Spendlove, S., and Pasaniuc, B. (2017). Local genetic correlation gives insights into the shared genetic architecture of complex traits. Am. J. Hum. Genet. *101*, 737–751.
55. Watanabe, K., Taskesen, E., Van Bochoven, A., and Posthuma, D. (2017). Functional mapping and annotation of genetic associations with FUMA. Nat. Commun. *8*, 1826–1911. https://doi.org/10.1038/s41467-017-01261-5.
56. de Leeuw, C.A., Mooij, J.M., Heskes, T., Posthuma, D., Visscher, P., Brown, M., McCarthy, M., Yang, J., Manolio, T., Collins, F., et al. (2015). MAGMA: generalized gene-set analysis of GWAS data. PLoS Comput. Biol. *11*, e1004219. https://doi.org/10.1371/journal.pcbi.1004219.
57. Barbeira, A.N., Dickinson, S.P., Bonazzola, R., Zheng, J., Wheeler, H.E., Torres, J.M., Torstenson, E.S., Shah, K.P., Garcia, T., Edwards, T.L., et al. (2018). Exploring the phenotypic consequences of tissue specific gene expression variation inferred from GWAS summary statistics. Nat. Commun. *9*, 1825–1920. https://doi.org/10.1038/s41467-018-03621-1.
58. Langfelder, P., and Horvath, S. (2008). WGCNA: an R package for weighted correlation network analysis. BMC Bioinformatics *9*, 559. https://doi.org/10.1186/1471-2105-9-559.
59. Ge, T., Chen, C.-Y., Ni, Y., Feng, Y.-C.A., and Smoller, J.W. (2019). Polygenic prediction via Bayesian regression and continuous shrinkage priors. Nat. Commun. *10*, 1776. https://doi.org/10.1038/s41467-019-09718-5.
60. Chang, C.C., Chow, C.C., Tellier, L.C.A., Vattikuti, S., Purcell, S.M., and Lee, J.J. (2015). Second-generation PLINK: Rising to the challenge of larger and richer datasets. GigaScience *4*, 7. https://doi.org/10.1186/s13742-015-0047-8.
61. Sheng, Y., and Wikle, C.K. (2008). Bayesian multidimensional IRT models with a hierarchical structure. Educ. Psychol. Meas. *68*, 413–430.
62. Altshuler, D.M., Gibbs, R.A., Peltonen, L., Altshuler, D.M., Dermitzakis, E., Schaffner, S.F., Yu, F., Dermitzakis, E., Bonnen, P.E., de Bakker, P.I.W., et al. (2010). Integrating common and rare genetic variation in diverse human populations. Nature *467*, 52–58. https://doi.org/10.1038/nature09298.
63. Hu, L., and Bentler, P.M. (1999). Cutoff criteria for fit indexes in covariance structure analysis: conventional criteria versus new alternatives. Struct. Equation Model. a multidisciplinary J. *6*, 1–55.
64. Auton, A., Abecasis, G.R., Brooks, L.D., Durbin, R.M., Garrison, E.P., Kang, H.M., Korbel, J.O., Marchini, J.L., McCarthy, S., McVean, G.A., et al. (2015). A global reference for human genetic variation. Nature *526*, 68–74. https://doi.org/10.1038/nature15393.
65. Cai, N., Revez, J.A.A., Adams, M.J., Andlauer, T.F.M., Breen, G., Byrne, E.M., Clarke, T.-K., Forstner, A.J.J., Grabe, H.J.J., Hamilton, S.P., et al. (2019). Minimal phenotyping yields gwas hits of reduced specificity for major depression. Preprint at BioRxiv, 440735. https://doi.org/10.1101/440735.
66. Wang, K., Li, M., and Hakonarson, H. (2010). ANNOVAR: functional annotation of genetic variants from high-throughput sequencing data. Nucleic Acids Res. *38*, e164. https://doi.org/10.1093/nar/gkq603.
67. Aguet, F., Barbeira, A.N., Bonazzola, R., Brown, A., Castel, S.E., Jo, B., Kasela, S., Kim-Hellmuth, S., Liang, Y., Oliva, M., et al. (2019). The GTEx Consortium Atlas of Genetic Regulatory Effects across Human Tissues. Preprint at BioRxiv, 787903. https://doi.org/10.1126/2Fscience.aaz1776.
68. Giusti-Rodriguez, P.M.D., and Sullivan, P.F. (2019). Using three-dimensional regulatory chromatin interactions from adult and fetal cortex to interpret genetic results for psychiatric disorders and cognitive traits. Preprint at BioRxiv, 406330. https://doi.org/10.1101/406330.
69. Zhao, B., Luo, T., Li, T., Li, Y., Zhang, J., Shan, Y., Wang, X., Yang, L., Zhou, F., Zhu, Z., and Zhu, H. (2019). Genome-wide association analysis of 19,629 individuals identifies variants influencing regional brain volumes and refines their genetic co-architecture with cognitive and mental health traits. Nat. Genet. *51*, 1637–1644. https://doi.org/10.1038/s41588-019-0516-6.
70. Watanabe, K., Stringer, S., Frei, O., Umićević Mirkov, M., de Leeuw, C., Polderman, T.J.C., van der Sluis, S., Andreassen, O.A., Neale, B.M., and Posthuma, D. (2019). A global overview of pleiotropy and genetic architecture in complex traits. Nat. Genet. *51*, 1339–1348. https://doi.org/10.1038/s41588-019-0481-0.
71. Hawrylycz, M.J., Lein, E.S., Guillozet-Bongaarts, A.L., Shen, E.H., Ng, L., Miller, J.A., Van De Lagemaat, L.N., Smith, K.A., Ebbert, A., Riley, Z.L., et al. (2012). An anatomically comprehensive atlas of the adult human brain transcriptome. Nature *489*, 391–399. https://doi.org/10.1038/nature11405.
72. Klein, A., and Tourville, J. (2012). 101 labeled brain images and a consistent human cortical labeling protocol. Front. Neurosci. *6*, 171. https://doi.org/10.3389/fnins.2012.00171.
73. Romero-Garcia, R., Whitaker, K.J., Váša, F., Seidlitz, J., Shinn, M., Fonagy, P., Dolan, R.J., Jones, P.B., Goodyer, I.M., Bullmore, E.T., and Vertes, P.E. (2018). Structural covariance networks are coupled to expression of genes enriched in supragranular layers of the human cortex. Neuroimage *171*, 256–267. https://doi.org/10.1016/j.neuroimage.2017.12.060.

STAR★METHODS

KEY RESOURCES TABLE

REAGENT or RESOURCE	SOURCE	IDENTIFIER
Deposited data		
Summary statistics for multivariate GWAS of F1 & F2	This study	https://osf.io/jm3y6/
Summary statistics for individual psychiatric symptoms	This study	https://osf.io/jm3y6/
Summary statistics for individual psychiatric disorders	Psychiatric Genomics Consortium	https://www.med.unc.edu/pgc/download-results/
Individual-level data from UK Biobank	UK Biobank	https://biobank.ndph.ox.ac.uk/showcase/
Genotype reference panel	1000 Genomes Project	http://hgdownload.soe.ucsc.edu/downloads.html#human
European LD scores and weights	Broad Institute	https://alkesgroup.broadinstitute.org/LDSCORE/
Developmental postmortem brain gene expression data	PsychENCODE	http://development.psychencode.org#
Adult postmortem brain gene expression data	Allen Human Brain Atlas	https://human.brain-map.org/static/download
Software and algorithms		
M*plus*	[48]	https://www.statmodel.com
BOLT-LMM	[49]	https://alkesgroup.broadinstitute.org/BOLT-LMM/downloads/
flashPCA2	[50]	https://github.com/gabraham/flashpca
EasyQC	[51]	https://www.uni-regensburg.de/medizin/epidemiologie-praeventivmedizin/genetische-epidemiologie/software
Genomic SEM	[19]	https://github.com/GenomicSEM/GenomicSEM
LD score regression	[52]	https://github.com/bulik/ldsc
HESS	[53]	https://github.com/huwenboshi/hess
ρ-HESS	[54]	https://github.com/huwenboshi/hess
FUMA	[55]	https://fuma.ctglab.nl
MAGMA	[56]	https://ctg.cncr.nl/software/magma
S-PrediXcan	[57]	https://github.com/hakyimlab/MetaXcan
WGCNA	[58]	https://cran.r-project.org/web/packages/WGCNA/index.html
PRS-CS	[59]	https://github.com/getian107/PRScs
PLINK	[60]	https://www.cog-genomics.org/plink/

RESOURCE AVAILABILITY

Lead contact

Any inquiries about analytical results or other information should be directed to lead contact, Travis T. Mallard (tmallard@mgh.harvard.edu).

Materials availability

No new materials were generated as part of this study.

Data and code availability

This paper analyzes existing, publicly available data. These accession numbers for the datasets are listed in the key resources table. This paper does not report custom code or software. Any additional information required to reanalyze the data reported in this paper is available from the lead contact upon request.

METHOD DETAILS

Phenotype construction in UK biobank

M*plus*[48] v8 was used to estimate person-specific thetas (*i.e.*, factor scores) for three symptom domains: depression, mania, and psychosis. As each psychiatric phenotypes was assessed by four items, thetas were estimated via a multidimensional two-parameter probit model,[61] which allowed item-level responses across measurement occasions to be combined for correlated latent variables

simultaneously. Furthermore, a combination of multiple imputation and Bayesian estimation with non-informative priors was used to maximally leverage all available responses for participants to minimize the impact of missing data. See Section 1.1 of Methods S1 for further description of the phenotypic modeling.

Univariate genome-wide association analyses

BOLT-LMM[49] v2.3.2 was used to conduct GWASs in the UK Biobank for three lifetime measures of psychiatric symptoms: depression, mania, and psychosis. This approach used a linear mixed model that included a genetic relationship matrix to estimate SNP effects, which offered improved control for population stratification and maximized power by accounting for relatedness among individuals. The first 40 principal components of ancestry computed with flashPCA2 (Section 1.2 of Methods S1), sex, birth year, sex-by-birth year interactions, and batch were included as covariates. EasyQC[51] was used to perform extensive quality control on the GWAS summary statistics. The main objective of the quality control was to filter out rare and low-frequency SNPs, as well as SNPs that were not imputed well. Three main filters were imposed: (i) MAF <0.005; (ii) imputation quality score <0.9; (iii) unavailable in reference panel. Additional quality control procedures and filters are further described in Section 1.3 of Methods S1. The reference panel was a combination of the 1000 Genomes phase 3 v5 and UK10K, which has been described in a previous study.[14]

Multivariate genome-wide association analyses

Genomic SEM[19] v0.0.2 was used to conduct multivariate GWAS based on eight phenotypes: depressive symptoms, manic symptoms, psychotic symptoms, major depressive disorder, bipolar II disorder, bipolar I disorder, schizoaffective disorder, and schizophrenia (see Table 1 for overview). Following identification of the confirmatory factor model that best explained the observed genetic covariances among the phenotypes, Genomic SEM was used to estimate the individual SNP effects on each latent factor in the model. Note that Genomic SEM is unbiased in the presence of varying and unknown sample overlap across the contributing GWAS samples, as the cross-trait intercepts estimated via multivariable LD score regression are used to estimate (and account for) sample overlap and phenotypic correlation.

Effective sample size (N_{eff}) for each latent factor was estimated as $N_{eff} \approx \frac{1}{m}\sum_{a}^{b} n_j$, where m is the number of SNPs in the GWAS, a is the lower MAF threshold for inclusion in the calculation (here, 10%), b the upper limit (here, 40%), and n_j is the effective sample size for SNP j, which is calculated as $(Z_j/\beta_j)^2/\sigma_j^2$. Q_{SNP} tests were used to evaluate whether SNP effects on the latent factors were driven by heterogeneous effects across constituent phenotypes. Further description of multivariate association analyses and Q_{SNP} tests is provided in Sections 2.4 and 2.5 of Methods S1, respectively.

Genetic correlations among study phenotypes

LD score regression[52] v1.0.1 was used to estimate genetic correlations between all pairwise combinations of the eight study phenotypes. Standard procedures and best practices for LD score regression were followed (*e.g.*, restricting to HapMap3[62] SNPs with a minor allele frequency $\geq$0.01). Default parameters were used for the three new GWASs of psychiatric symptoms. For the existing GWASs of psychiatric disorders, parameters (*e.g.*, sample prevalence, population prevalence) were defined as outlined in the original studies. A hierarchical clustering algorithm was applied to the final genetic correlation matrix to guide factor selection in the exploratory factor analysis. Although the original LD score regression software was used for this preliminary analysis, the multivariable version of LD score regression employed by Genomic SEM was used for all subsequent analyses. Please note that these software produce estimates that are effectively identical.

Exploratory factor analysis

The stats R package was used to conduct an EFA of the genetic correlations among the eight study phenotypes. Specifically, the *factanal* function was used to conduct an EFA with promax rotation on the standardized S matrix derived from the multivariable version of LD score regression employed by Genomic SEM. This enabled an empirical assessment of (i) the number of latent factors that best explained the multivariate genetic architecture observed among the set of study phenotypes (*i.e.*, the number of transdiagnostic liabilities present), and (ii) how constituent phenotypes load onto separable latent factors. As suggested by the hierarchical clustering algorithm, two factors were extracted that optimally accounted for shared variation among sets of the observed variables. Results from this analysis were subsequently used to guide construction of the confirmatory factor models. A brief overview of factor analysis is provided in Section 2.2 of Methods S1.

Confirmatory factor analysis

Genomic SEM was used to test whether a common factor model or a correlated factors model best fit the data via CFA, where fit reflects the degree to which the specified latent variable structure adequately explains the observed covariances among the set of observed variables. Parameter estimates were derived using weighted least squares estimation. Model fit was assessed using conventional indices in structural equation modeling: the model χ^2 statistic, the Akaike information criterion (AIC), the comparative fit index (CFI), and the standardized root mean square residual (SRMR). All fit indices retain their standard interpretations within a Genomic SEM framework. However, the model χ^2 statistic is best used as a comparative measure of fit to evaluate competing

models rather than a measure of statistical significance given the sensitivity of model χ^2 to sample size, which is comparatively extremely large for GWAS samples. For CFI and SRMR, values greater than .90 and less than .08, respectively, were considered reflective of good model fit.[63] Further description of structural equation modeling and confirmatory factor analysis are provided in Section 2.3 of Methods S1.

Heritability for observed and latent phenotypes

LD score regression was used to estimate the heritability of the three psychiatric symptom phenotypes, as well as the two latent genetic factors. Standard procedures and best practices for LD score regression were followed. As there is no phenotypic variance for latent genetic factors modeled in Genomic SEM, heritability is more accurately referred to as genetic variance for F1 and F2. Furthermore, as genetic variance estimates are influenced by the heritability estimates of constituent phenotypes and the metric of the latent genetic factor, we note that estimates for F1 and F2 should only be interpreted in the context of the present study.

Local heritability and genetic correlations

HESS[53] and its bivariate extension, ρ-HESS,[54] were used to estimate local genetic variance, local genetic covariance, and the proportion of the genome that contributes to the total genetic covariance for F1 and F2. For each factor, HESS was first used to estimate local genetic variance and covariance across 1,698 approximately LD-independent contiguous genomic partitions, averaging 1.5 Mb per partition. The European samples from the 1000 Genomes Project Phase 3v5[64] (n = 503) were used as a reference panel for these analyses. Independent genomic partitions were then ranked by their absolute genetic covariance, and the percentage that accounted for 80% of the total genetic covariance between F1 and F2 was used to further quantify genetic overlap between F1 and F2.[65]

Gene mapping and identification

The FUMA[55] SNP2GENE pipeline was used to apply a standard clumping algorithm that identified associated genomic loci, lead SNPs within loci, and all independent significant SNPs within loci. The European samples from the 1000 Genomes Project Phase 3v5 (n = 503) were used as a reference panel for LD. FUMA was also used to employ an ensemble of methods to identify putative risk genes for the univariate and multivariate GWAS phenotypes. Specifically, FUMA v1.3.6c was used to conduct positional, eQTL, and chromatin interaction mapping to identify risk-conferring genes that map to genome-wide significant loci. Default parameters were used for each of these analyses. ANNOVAR annotations[66] were used for positional mapping, the Geno-type-Tissue Expression (GTEx) v8 brain dataset[67] was used as the reference tissue data for eQTL mapping, and Hi-C data from adult and fetal human brain samples[68] was used to examine enhancer-promoter and promoter-promoter chromatin interactions.

Two additional methods were employed to identify putative risk genes based on genome-wide summary statistics: and MAGMA[56] and S-PrediXcan.[57] The former was used to calculate gene-based association statistics, and the latter was used to identify functionally expressed genes via joint analysis of SNP effects and eQTL expression effects. Both methods are described in the following section.

Gene-based association and enrichment analyses

MAGMA v1.08, a bioinformatics software for gene-based biological annotation, was used to conduct gene association, gene set enrichment, and gene property analyses for all novel study phenotypes. Default MAGMA parameters were employed and standard procedures were followed for gene-based association analyses based on summary statistics. MAGMA was also used to conduct competitive gene-set enrichment and gene property analyses based on the gene-level p values produced in the association analyses. These analyses tested whether genes within an annotated set are more strongly associated with the phenotype of interest than other genes. For gene set enrichment analyses, up to 9,987 gene sets cataloged in MolSigDB v7.0 were tested, which corresponded to 7,343 biological processes, 1,001 cellular components, and 1,643 molecular functions. For the gene property analyses, 54 tissues from the GTEx v8 dataset were tested. Bonferroni-corrected thresholds of $p \leq 5.01e\text{-}6$ and $p \leq 9.26e\text{-}4$ were used to determine significance for gene sets and tissues, respectively.

S-PrediXcan v0.6.2 was used (i) to predict gene expression levels in brain tissues, and (ii) to test whether predicted gene expression correlated with either transdiagnostic factor. Tissue weights were computed using reference data from the GTEx v8 dataset. GWAS summary statistics for F1 and F2, the reference transcriptomic data, and covariance matrices for the SNPs within each gene model were included as input data. Thirteen brain tissues were tested: anterior cingulate cortex, amygdala, caudate basal ganglia, cerebellar hemisphere, cerebellum, cortex, frontal cortex, hippocampus, hypothalamus, nucleus accumbens basal ganglia, putamen basal ganglia, spinal cord and substantia nigra. A Bonferonni-corrected threshold of $p \leq 8.97e\text{-}7$ was established for transcriptome-wide significance, which corrected for 55,753 gene-based tests.

Genetic correlation analyses between latent factors and other complex traits

Genomic SEM was used to estimate genetic correlations and partial genetic correlations between latent factors of psychopathology and other phenotypes of interest. Specifically, genetic correlations were estimated for two broad sets of phenotypes: (i) morphological features of the human brain, and (ii) complex traits related to human health and well-being. Summary statistics for 101 neuroimaging phenotypes[69] (cortical and subcortical gray matter volumes, ventricular volumes, and global measures of brain

volume) were downloaded from https://github.com/BIG-S2/GWAS. Summary statistics for 92 phenotypes broadly related to various domains of human health and well-being were downloaded from various online sources, using download links from GWAS Atlas[70] whenever possible. All summary statistics were cleaned and processed using the *munge* function of Genomic SEM, retaining all HapMap3 SNPs outside of the major histocompatibility complex regions with an allele frequency $\geq$ .01. A Bonferroni correction was applied within each family of tests to adjust p values for multiple comparisons ($p \leq 4.95e\text{-}4$ for neuroimaging phenotypes; $p \leq 5.43e\text{-}4$ for complex traits).

Spatiotemporal transcriptomic analyses

Microarray gene expression data from the Allen Human Brain Atlas (AHBA)[71] were downloaded from https://human.brain-map.org/static/download, and subsequently aligned to the Desikan-Killiany-Tourville atlas ($N = 62$ cortical brain regions)[72] for spatial compatibility with the cortical neuroimaging phenotypes.[73] Spatial correlation coefficients (Spearman's ρ) were computed for each of 20,647 genes compared against the $-\log_{10}$ p values from F1 and F2. To examine the developmental trajectories of the F1 and F2 gene sets (positive *Z*-scores of AHBA correlation coefficients, $p < .05$), weighted gene correlation network analysis[58] was used to estimate eigengene values (i.e., gene set expression) for these gene sets in the PsychENCODE dataset, treating each factor-specific gene set as a module. These expression values were then plotted as function of time, using a non-parametric LOESS curve line-of-best-fit to characterize developmental expression trajectories for F1 and F2, which indicated that the prioritized gene sets for each transdiagnostic factor are differentially expressed in pre- and postnatal cortical tissue. Evaluation of cell-type-specific gene sets was performed as above, using available data from a recent cell-specific sequencing study in adult human brain tissue.[25]

Phenome-wide polygenic prediction

PRS-CS[59] and PLINK[60] v1.9 were used to calculate polygenic scores for the transdiagnostic latent genetic factors, F1 and F2. PRS-CS, a Bayesian polygenic prediction method, was used to apply a continuous shrinkage prior to SNP effect estimates and infer posterior SNP weights using GWAS summary statistics for F1 and F2 and an external reference panel to model LD. In the present study, PRS-CS was used to adjust weights for 1,027,871 SNPs typed on both the 1000 Genomes Project Phase 3v5 and the HapMap3 reference panels with a minor allele frequency $\geq$ .01. The European samples from the 1000 Genomes Project Phase 3v5 (n = 503) were used as a reference panel for LD. PLINK was then used to calculate polygenic scores for each individual by summing all included variants weighted by the inferred posterior effect size for the effect allele, and converting that value to a Z-score for each participant within the prediction sample.

The genotyped BioVU sample (n = 66,915) was used to test for associations between polygenic scores for F1 and F2 and a wide array of medical phenotypes. Genotyping and quality control for this sample have been described elsewhere. Case-control medical phenotypes, also referred to as "phecodes," were constructed from International Classification of Disease (ICD) diagnostic codes in participant electronic health record data. Two instances of an ICD diagnostic code were required to be present to be classified as a case for a given phecode, and 50 cases were required for a phecode to be analyzed. A total of 1,335 phecodes were included in the phenome-wide association analyses. The PheWAS R package was used to conduct phenome-wide association analyses. A logistic regression model was fit to each of 1,335 case/control phenotypes to estimate the odds of each diagnosis given the polygenic scores for F1 and F2. Sex, median age of the longitudinal electronic health record measurements, and the top 10 principal components of ancestry were included as covariates. A Bonferroni-corrected threshold of at $p \leq 3.74e\text{-}5$ was established for phenome-wide significance.

Cell Genomics, Volume *2*

Supplemental information

Multivariate GWAS of psychiatric disorders and their cardinal symptoms reveal two dimensions of cross-cutting genetic liabilities

Travis T. Mallard, Richard Karlsson Linnér, Andrew D. Grotzinger, Sandra Sanchez-Roige, Jakob Seidlitz, Aysu Okbay, Ronald de Vlaming, S. Fleur W. Meddens, Bipolar Disorder Working Group of the Psychiatric Genomics Consortium, Abraham A. Palmer, Lea K. Davis, Elliot M. Tucker-Drob, Kenneth S. Kendler, Matthew C. Keller, Philipp D. Koellinger, and K. Paige Harden

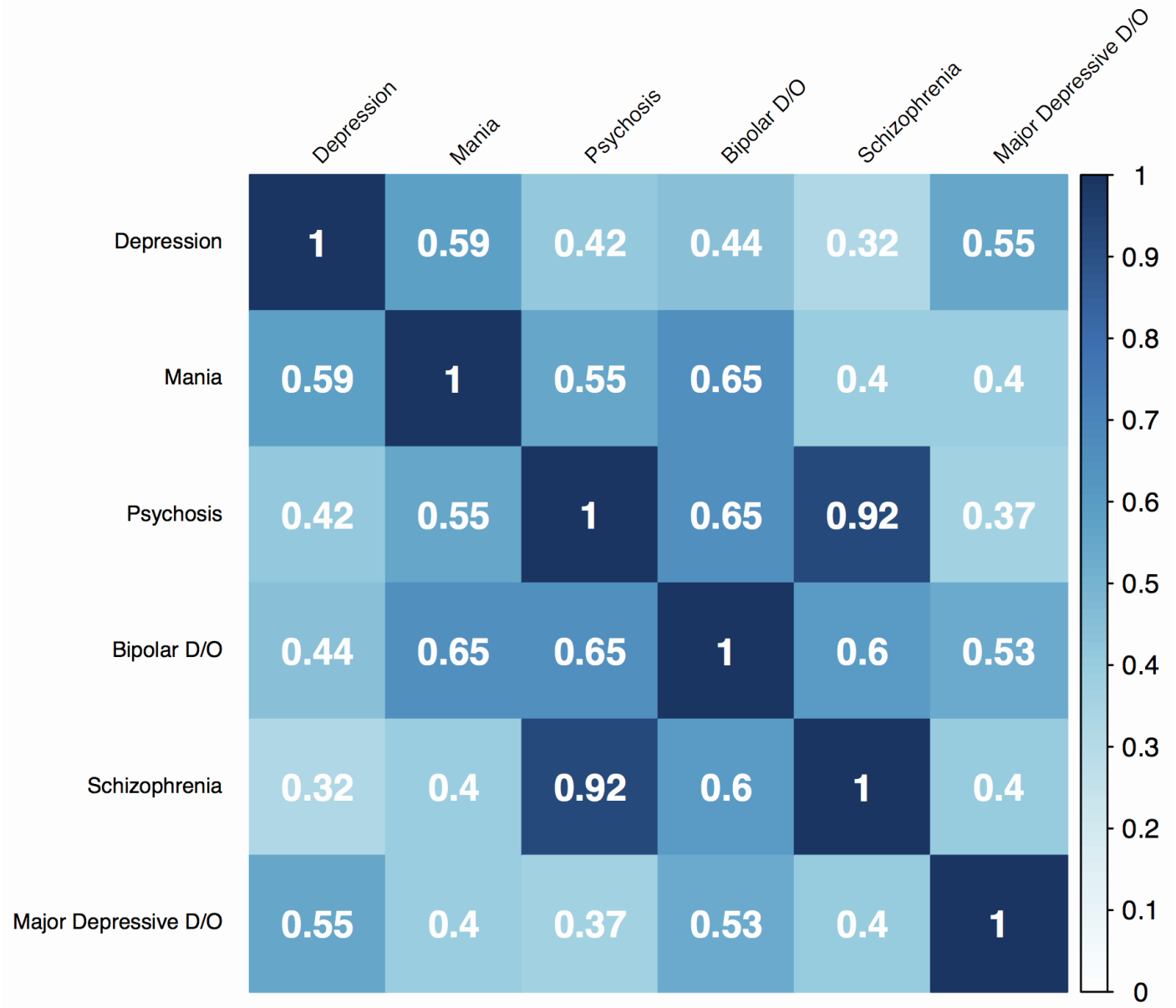

Figure S1. Phenotypic correlations between psychiatric symptoms and disorders, related to Figure 2. Matrix of phenotypic correlations for available psychiatric symptoms and disorders in the UK Biobank discovery sample.

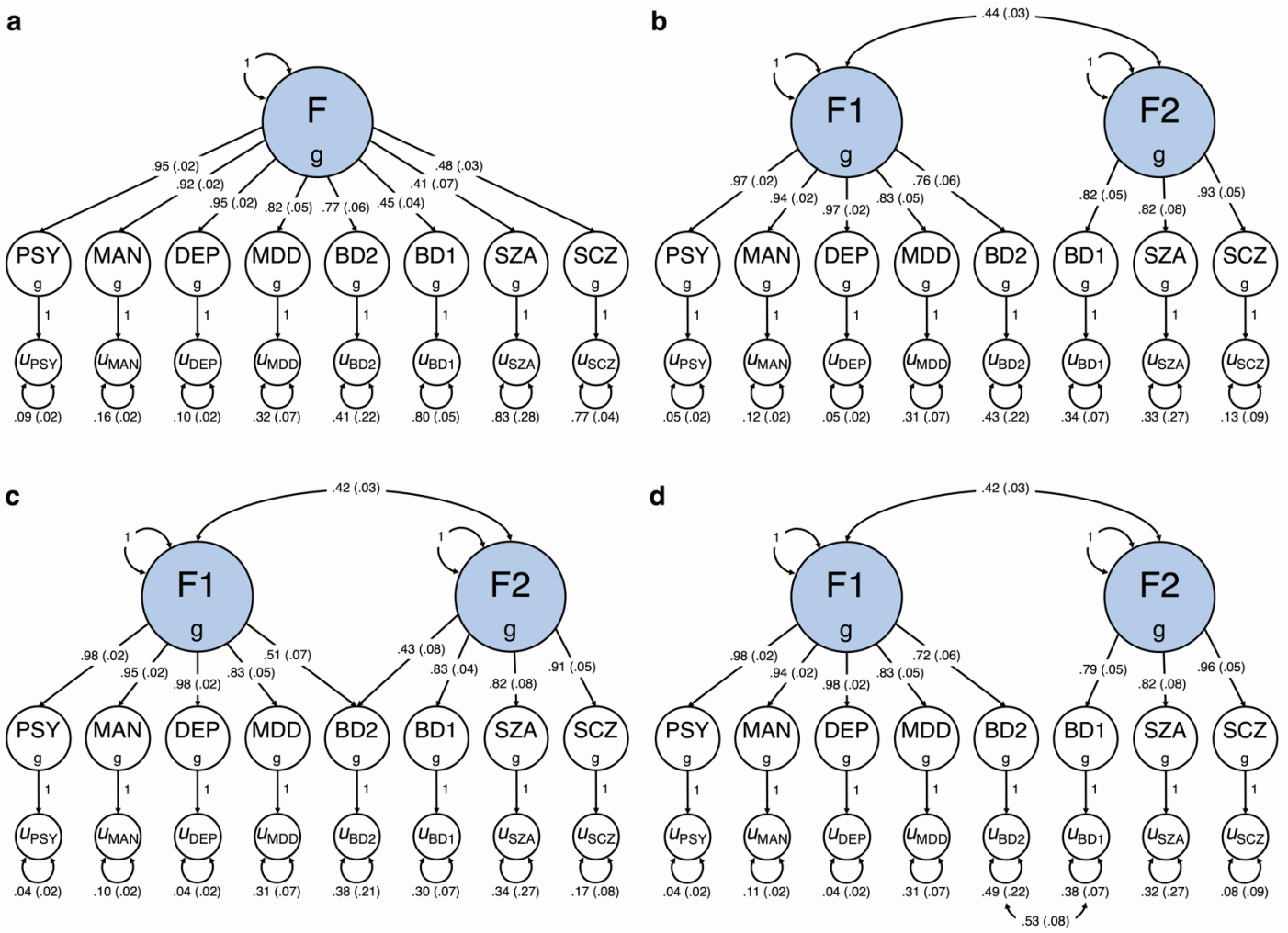

Figure S2. Path diagrams for the four confirmatory factor models, related to Figure 2. a,**b**,**c**,**d,** Path diagrams with standardized parameter estimates for (**a**) a common factor model, (**b**) a correlated factors model, (**c**) a correlated factors model with bipolar II disorder cross-loading on both factors, and (**d**) a correlated factors model with correlated residuals between bipolar I disorder and bipolar II disorder. Standard errors are reported in parentheses next to each parameter estimate. Latent genetic factors are highlighted in blue.

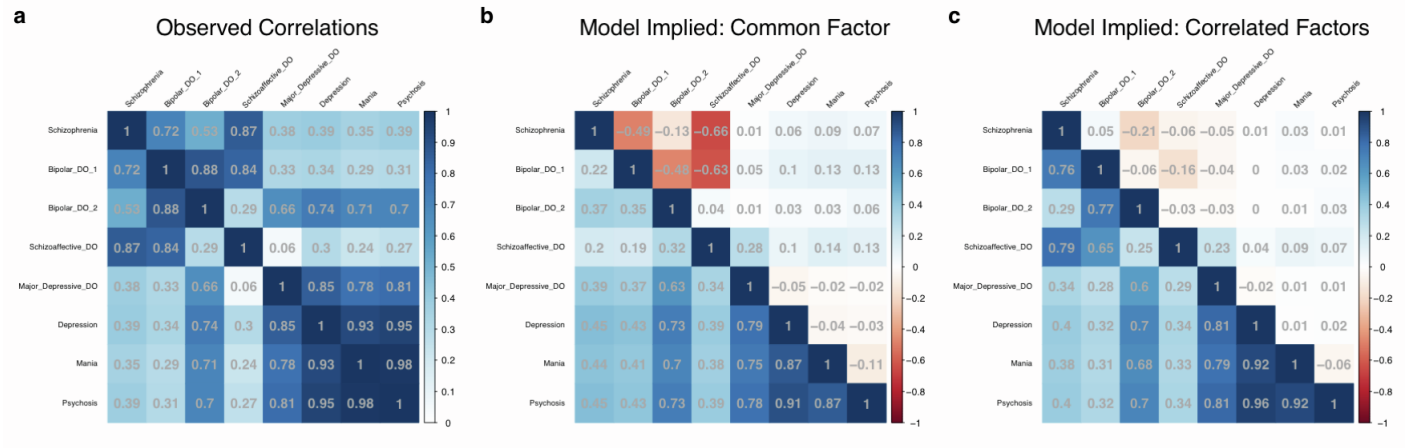

Figure S3. Observed and implied genetic correlation matrices, related to Figure 2. a, Matrix of observed genetic correlations for the eight psychiatric symptoms and disorders. **b**,**c**, Matrices of model implied genetic correlations for (**a**) the common factor (*i.e.*, the *p* factor) and (**b**) the final correlated factors model (Figure S2d). Model implied correlations are presented below the diagonal while the difference between the model implied and observed correlations (model implied r_g – observed r_g) are presented above the diagonal. Positive and negative values above the diagonal, therefore, reflect upwardly and downwardly biased estimates, respectively.

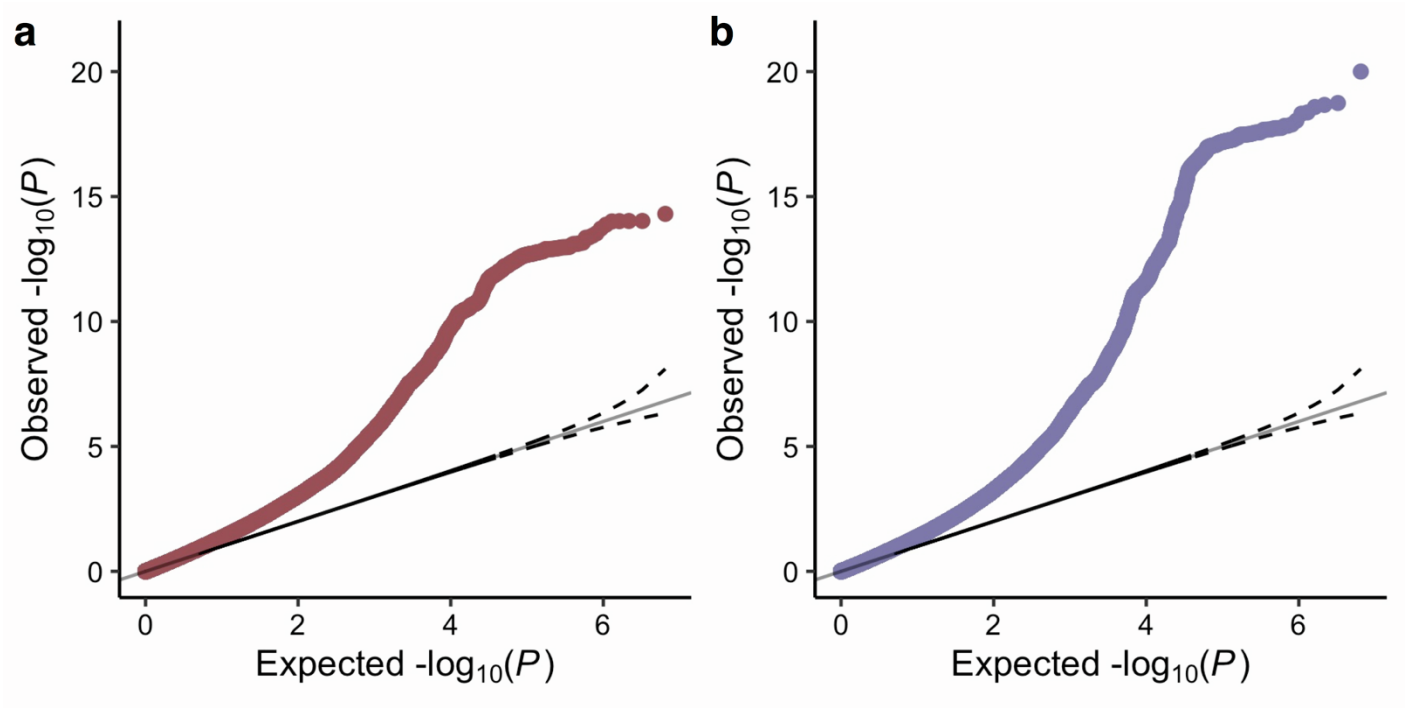

Figure S4. Quantile-quantile plot for the latent genetic factors, related to Figure 3. a,**b**, Quantile-quantile plot for (**a**) F1 and (**b**) F2, illustrating strong polygenic signal for both multivariate GWAS. The y-axis corresponds to the observed distribution of *P*, while the x-axis corresponds to the expected distribution of *P* under the null. The null is plotted as a solid gray line, and the accompanying 95% confidence interval is plotted as a dotted black line.

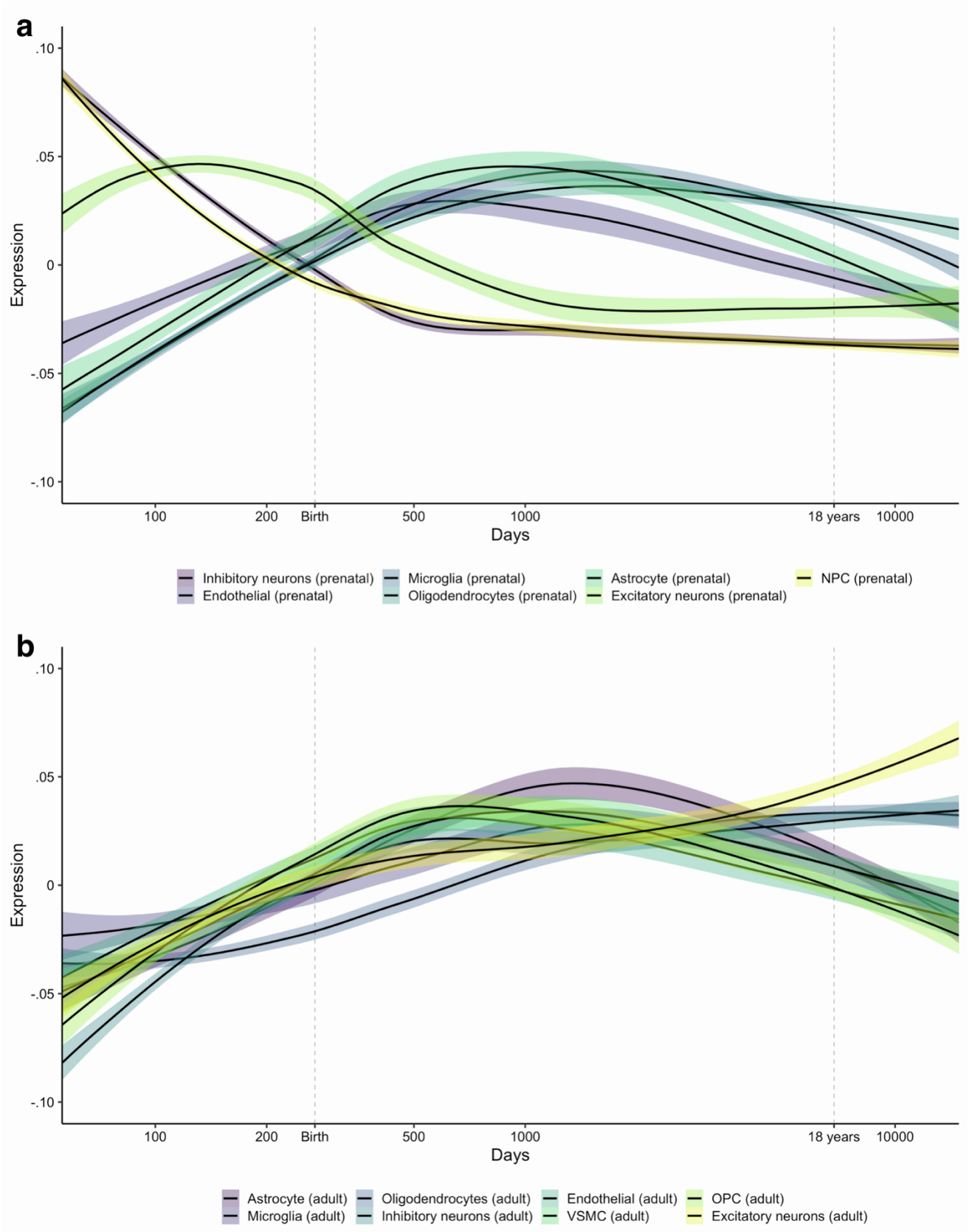

Figure S5. Spatiotemporal gene expression of specific cell types, related to Figure 4. a,**b**, Developmental trajectories fit via LOESS regression for (**a**) prenatal and (**b**) adult cell types in the Brainspan dataset. Cell type data is derived from Li and colleagues[10]. Note: inhibitory neurons = mostly GABAergic interneurons, excitatory neurons = mostly glutamatergic excitatory projection neurons, NPC = neural progenitor cells, VSMC = vascular smooth muscle cells, OPC = oligodendrocyte progenitor cells.

Methods S1, Supplemental description of methods employed in this study, related to STAR Methods.

Multivariate GWAS of psychiatric disorders and their cardinal symptoms reveal two dimensions of cross-cutting genetic liabilities

Travis T. Mallard[a,1,2], Richard Karlsson Linnér[3,4], Andrew D. Grotzinger[1], Sandra Sanchez-Roige[5,6], Jakob Seidlitz[7,8], Aysu Okbay[3], Ronald de Vlaming[3], S. Fleur W. Meddens[9], Bipolar Disorder Working Group of the Psychiatric Genomics Consortium, Abraham A. Palmer[5,10], Lea K. Davis[6,11,12], Elliot M. Tucker-Drob[1,13], Kenneth S. Kendler[14,15], Matthew C. Keller[16,17], Philipp D. Koellinger[b,3], & K. Paige Harden[b,1,13]

[a]Lead Contact
[b]Senior Author

Affiliations:

1. Department of Psychology, University of Texas at Austin, Austin, TX, USA
2. Psychiatric and Neurodevelopmental Genetics Unit, Center for Genomic Medicine, Massachusetts General Hospital, Boston, MA
3. Department of Economics, School of Business and Economics, Vrije Universiteit Amsterdam, Amsterdam, The Netherlands
4. Autism and Developmental Medicine Institute, Geisinger, Lewisburg, PA, USA
5. Department of Psychiatry, University of California San Diego, La Jolla, CA, USA
6. Department of Medicine, Vanderbilt University Medical Center, Nashville, TN, USA
7. Department of Child and Adolescent Psychiatry and Behavioral Science, Children's Hospital of Philadelphia, Philadelphia, PA, USA
8. Department of Psychiatry, University of Pennsylvania, Philadelphia, PA, USA
9. Erasmus University Rotterdam Institute for Behavior and Biology, Erasmus School of Economics, Erasmus University Rotterdam, Rotterdam, The Netherlands
10. Institute for Genomic Medicine, University of California San Diego, La Jolla, CA, USA
11. Department of Biomedical Informatics, Vanderbilt University Medical Center, Nashville, TN, USA
12. Department of Psychiatry and Behavioral Sciences, Vanderbilt University Medical Center, Nashville, TN, USA
13. Population Research Center, University of Texas at Austin, Austin, TX USA
14. Virginia Institute for Psychiatric and Behavioral Genetics, Virginia Commonwealth University, Richmond, VA, USA
15. Department of Psychiatry, Medical College of Virginia/Virginia Commonwealth University, Richmond, VA, USA
16. Institute for Behavioral Genetics, University of Colorado Boulder, Boulder, CO, USA
17. Department of Psychology and Neuroscience, University of Colorado Boulder, Boulder, CO, USA

Correspondence to:

Travis T. Mallard, Ph.D., Center for Genomic Medicine, Massachusetts General Hospital, 185 Cambridge Street, Boston, MA 02114, USA. E-mail: tmallard@mgh.harvard.edu

K. Paige Harden, Ph.D., Department of Psychology, The University of Texas at Austin, 108 E. Dean Keeton Street, Stop A8000, Austin, TX 78712, USA. E-mail: harden@utexas.edu

Table of Contents

1 Genome-wide association analyses in UK Biobank

To investigate the genetic architecture of psychiatric symptoms related to mood disturbance and psychosis, we used a novel combination of Bayesian item response theory and linear mixed models to conduct univariate GWASs in the UK Biobank (N = 252,252). Details regarding the phenotypes and extensive quality control procedures are described below.

1.1 Phenotype construction

Lifetime symptoms of depression and mania were assessed with two sets of items administered via in-person (Wave 1) and online (Wave 2) surveys. Lifetime symptoms of psychosis were only assessed during the online follow-up survey. Although items were very similar across assessment occasions, there were slight differences in wording and response options, as described below.

1.1.1 Depression

Wave 1. The in-person surveys indexed depressive symptoms with two screener items that assessed the presence of notable, prolonged feelings of sadness or apathy.

1. "Looking back over your life, have you ever had a time when you were feeling depressed or down for at least a whole week?"
    - Data-Field 4598 (Data-Coding 100349).
    - Possible responses: "Yes", "No", "Do not know", and "Prefer not to answer".
2. "Have you ever had a time when you were uninterested in things or unable to enjoy the things you used to for at least a whole week?"
    - Data-Field 4631 (Data-Coding 100349).
    - Possible responses: "Yes", "No", "Do not know", and "Prefer not to answer".

Wave 2. The web-based follow-up survey also indexed depressive symptoms with two screener items that assessed the presence of notable, prolonged feelings of sadness or apathy

1. "Have you ever had a time in your life when you felt sad, blue, or depressed for two weeks or more in a row?"
    - Data-Field 4598 (Data-Coding 503).
    - Possible responses: "Yes", "No", and "Prefer not to answer".
2. "Have you ever had a time in your life lasting two weeks or more when you lost interest in most things like hobbies, work, or activities that usually give you pleasure?"
    - Data-Field 4631 (Data-Coding 503).
    - Possible responses: "Yes", "No", and "Prefer not to answer".

1.1.2 Mania

Wave 1. The in-person surveys indexed manic symptoms with two screener items that assessed the presence of notable, prolonged feelings of (hypo)mania or irritability.

1. "Have you ever had a period of time lasting at least two days when you were feeling so good, "high", excited or "hyper" that other people thought you were not your normal self or you were so "hyper" that you got into trouble?"
    - Data-Field 4642 (Data-Coding 100349).
    - Possible responses: "Yes", "No", "Do not know", and "Prefer not to answer".

2. "Have you ever had a period of time lasting at least two days when you were so irritable that you found yourself shouting at people or starting fights or arguments?"
    - Data-Field 4653 (Data-Coding 100349).
    - Possible responses: "Yes", "No", "Do not know", and "Prefer not to answer".

Wave 2. The web-based follow-up survey indexed manic symptoms with two screener items that assessed the presence of notable, prolonged feelings of (hypo)mania or irritability.

1. "Have you ever had a period of time when you were feeling so good, "high", excited or "hyper" that other people thought you were not your normal self or you were so "hyper" that you got into trouble?"
    - Data-Field 20501 (Data-Coding 502).
    - Possible responses: "Yes", "No", "Do not know", and "Prefer not to answer".
2. "Have you ever had a period of time when you were so irritable that you found yourself shouting at people or starting fights or arguments?"
    - Data-Field 20502 (Data-Coding 502).
    - Possible responses: "Yes", "No", "Do not know", and "Prefer not to answer".

1.1.3 Psychosis

Wave 2. The web-based follow-up survey assessed psychotic symptoms with four screener items. These items indexed various types of unusual beliefs and experiences that are indicative of psychosis or psychotic-like experiences.

1. “Did you ever see something that wasn't really there that other people could not see? Please do not include any times when you were dreaming or half-asleep or under the influence of alcohol or drugs.”
    - Data-Field 20471 (Data-Coding 502).
    - Possible responses: "Yes", "No", "Do not know", and "Prefer not to answer".
2. “Did you ever hear things that other people said did not exist, like strange voices coming from inside your head talking to you or about you, or voices coming out of the air when there was no one around? Please do not include any times when you were dreaming or half-asleep or under the influence of alcohol or drugs.”
    - Data-Field 20463 (Data-Coding 502).
    - Possible responses: "Yes", "No", "Do not know", and "Prefer not to answer".
3. “Did you ever believe that a strange force was trying to communicate directly with you by sending special signs or signals that you could understand but that no one else could understand (for example through the radio or television)? Please do not include any times when you were dreaming or half-asleep or under the influence of alcohol or drugs.”
    - Data-Field 20474 (Data-Coding 502).
    - Possible responses: "Yes", "No", "Do not know", and "Prefer not to answer".
4. “Did you ever believe that there was an unjust plot going on to harm you or to have people follow you, and which your family and friends did not believe existed? Please do not include any times when you were dreaming or half-asleep or under the influence of alcohol or drugs.”
    - Data-Field 20468 (Data-Coding 502).
    - Possible responses: "Yes", "No", "Do not know", and "Prefer not to answer".

1.1.4 Item response theory models

To construct psychiatric symptom phenotypes in UK Biobank, we used M*plus*[1] v8 to estimate a two-parameter probit multidimensional item response theory (IRT) model, which simultaneously combined self-report items across waves for each symptom dimension while leveraging all available information and accounting for the

correlations between dimensions. IRT scaling was used as it does not assume that all items are equivalently related to the underlying construct of interest, accommodates differences in the base rate of item endorsement, and does not assume that missing data are missing completely at random. The advantages of IRT scaling using full-information estimation over averaging proportion scores for incomplete longitudinal data is described in more detail in Curran and colleagues[2]. The two parameter probit multidimensional IRT model can be expressed as:

$$P(y_{vij} = 1 | \theta_{vi}, \alpha_{vj}, \gamma_{vj}) = \Phi(\alpha_{vj}\theta_{vi} - \gamma_{vj}) = \int_{-\infty}^{\alpha_{vj}\theta_{vi}-\gamma_{vj}} \frac{1}{\sqrt{2\pi}} e^{\frac{-t^2}{2}} dt$$

where *P* represents probability; y_{vij} is the observed response for binary item *j* for individual *i* in symptom dimension *v*; and θ_{vi}, α_{vj}, and γ_{vj} are scalar parameters that represent the latent construct hypothesized to underlie the observed item response patterns, item discrimination (*i.e.*, the degree to which the item discriminates between individuals in different regions on the latent continuum), and item difficulty (*i.e.*, the location where the item provides maximum information) for symptom dimension *v*. We freely estimated slope parameters for all items, and we modeled items as functions of single time-invariant, symptom-specific θ parameters.

We estimated IRT model parameters (α_{vj}, γ_{vj}, and θ_{vi}) using a Bayesian framework with non-informative priors and multiple imputation, which maximally leveraged all available responses for participants and minimized the impact of missing data. This approach is a full information approach that is asymptotically equivalent to maximum likelihood estimation. We imputed 100 plausible θ values for each participant to create a sampling distribution of θ for each symptom. The median values of these distributions were then used as the phenotype for the GWAS.

1.1.5 Phenotypic factor structure in UK Biobank

To evaluate the phenotypic factor structure of psychiatric symptoms and disorders characterized by mood disturbance and psychosis, we first created diagnostic phenotypes for the 252,252 individuals in the discovery sample, corresponding to diagnoses of major depressive disorder, bipolar disorder, schizoaffective disorder, and schizophrenia. These phenotypes were derived from electronic health records.

1. Diagnoses - main ICD-10
    - Data-Field 41202 (Data-Coding 19)
2. Diagnoses - secondary ICD-10
    - Data-Field 41204 (Data-Coding 19)

Due to low base rates, schizoaffective disorder and schizophrenia cases were combined. These variables were then included as observed variables in the multidimensional IRT model described in Supplementary Section 1.1.4. We first estimated the zero-order correlations between each pairwise combination of the psychiatric symptoms and disorders (Figure S1). To maintain consistency across phenotypic and genetic factor analyses, we then conducted an exploratory factor analysis of the covariance matrix for these phenotypes, where we tested one-, two-, and three-factor solutions using the *factanal* function of R. As described in Supplementary Section 2.2, we retained the highest dimensional solution where each factor explained at least 20% of the variance.

Here, the three-factor solution satisfied this criterion (F1 = 35%, F2 = 29%, F3 = 23%), yielding three factors that were each predominantly characterized by a psychiatric disorder and their cardinal symptom(s). Specifically, we found that the factors corresponded to the following phenotypes (with loadings ≥ .30):

- F1: schizophrenia (1.08), psychosis (.90), and bipolar disorder (.31)
- F2: bipolar disorder (.54), mania (1.10), and depression (.51)
- F3: major depressive disorder (1.10) and depression (.31)

Collectively, these results suggest that symptoms and disorders tend to correlate most strongly in a canonical fashion at the phenotypic level (*i.e.*, psychosis with schizophrenia, mania with bipolar disorder, depression with major depressive disorder).

1.2 Principal components of ancestry

Although the present analyses were limited to participants who self-reported non-Hispanic European descent, we sought to further account for cryptic relatedness and population stratification specific to this population. To this end, we used flashPCA2[3] to extract the first 40 principal components of ancestry in individuals who reported having non-Hispanic European ancestry.

We used an approach that broadly paralleled the original process used to estimate principal components of ancestry in the entire UKB dataset, as well as the default flashPCA2 recommendations as outlined by Abraham and colleagues in their online code repository (https://github.com/gabraham/flashpca). Specifically, we first generated a list of UKB participants that (i) were used in original PCA (*i.e.*, passed QC thresholds, pruned for kinship, etc.) and (ii) self-reported 'White British' ethnicity and have very similar genetic ancestry based on original PCA of the genotypes (as determined in the sample QC file provided by UKB investigators). We then extracted the hard genotype calls for those individuals and applied the recommended SNP-level QC thresholds (directly genotyped SNPs outside of long-range LD regions, minor allele frequency $\geq .01$, genotyping call rate $\geq .02$, missingness rate $\leq .05$, and a Hardy-Weinberg equilibrium threshold $\geq$ 5e-6). Next, we applied the recommended LD pruning thresholds to produce a sample of 322,886 individuals with 77,355 independent markers before estimating the first 40 principal components with flashPCA2. Principal component loadings for each SNP used in the analysis were computed, exported, and then used to project all remaining participants of non-Hispanic European ancestry (e.g., siblings not used in the original PCA, participants of White Irish ancestry, participants of White Scottish ancestry, etc.) onto the PCs, yielding a final set of PC scores for the entire subsample. Scatterplots of the principal component scores were then manually examined to identify potential ancestral outliers in the sample.

1.3 Quality control

We used an EasyQC[4] pipeline similar to the one reported by Linnér and colleagues[5] to check each set of UKB summary statistics for quality control problems. For each results file, we applied the following threshold in order.

1. We removed SNPs if either allele corresponded to a value other than “A”, “C”, “G”, or “T”.
2. We excluded SNPs if any of the following values were missing: *P* value, beta, standard error, effect allele frequency, sample size, and imputation accuracy (for imputed SNPs).
3. We excluded SNPs with values outside of permissible ranges (*e.g.*, negative or infinite standard errors, nonsensical *P* values, allele frequencies greater than 1 or below 0).
4. We dropped SNPs with minor allele frequencies less than .005.
5. We filtered out SNPs with low imputation accuracy, which was defined as an imputation score < .90.
6. We dropped duplicated SNPs based on GRCh37 base pair positions. When duplicated SNPs were identified, we retained the SNP with the largest sample size.

We then inspected several diagnostic plots to further ensure that results were not prone to systematic errors, including:

7. We checked for errors in allele frequencies and strand orientations by inspecting a plot of allele frequencies in our analytic sample against the allele frequency in a non-Hispanic European reference sample.
8. We checked for discrepancies between the reported *P* values and the reported coefficient estimates and their SEs.
9. We looked for evidence of population stratification that had not been accounted for by checking a Q-Q plot.

2 Genomic structural equation modeling

Genomic structural equation modeling (Genomic SEM)[6] is a novel statistical method for applying structural equation modeling techniques to GWAS summary statistics to model the joint genetic architecture of complex traits. It is a flexible framework that allows for more accurate modeling of multivariate genetic covariance matrices, such as those derived from LD Score regression. Here, we conducted a series of Genomic SEM analyses to investigate the multivariate genetic architecture of the psychiatric symptoms and disorders characterized by mood disturbance and psychosis. The aim of these analyses is three-fold: (i) to identify the latent genetic factor(s) that best represent the factor structure of these phenotypes, (ii) to estimate the effects of individual SNPs on the latent genetic factor(s), and (iii) to evaluate heterogeneous effects among the discovery phenotypes.

2.1 Hierarchical clustering

Hierarchical clustering is a form of cluster analysis that aims to identify features of a dataset that are similar to one another. It serves as a precursor to factor analysis or structural equation modeling, as its results can be used guide model specification decisions in subsequent analyses. To this end, we applied a hierarchical clustering algorithm to a genetic correlation matrix of our eight psychiatric phenotypes prior to any form of factor analysis. Specifically, we applied the complete-linkage hierarchical clustering algorithm employed by the *hclust* function of R. The algorithm identified two clusters present in the matrix.

The first cluster was comprised of the symptom-level phenotypes (depression, mania, and psychosis), major depressive disorder, and bipolar II disorder. The second cluster was comprised of bipolar I disorder, schizoaffective disorder, and schizophrenia. Beyond these two clusters, there clear evidence of a positive manifold across all items. All point estimates were positive, and all but two of the 28 pairwise genetic correlations were significant following Bonferroni correction.

2.2 Factor analysis

Factor analysis is a multivariate statistical technique used to explain variance and covariance among sets of observed, correlated variables in terms of unobserved latent factors. It is a powerful tool for reducing dimensionality of data and accounting for measurement error in observed variables, often used in structural equation modeling. In factor analysis of genetic covariance matrices, k observed variables are described as linear functions of m latent variables, such that the model can be expressed as

$$y = \Lambda\eta + \varepsilon$$

where y is a $k \times 1$ vector of observed variables, ε is a $k \times 1$ vector of observed variable residuals, η is a $m \times 1$ vector of latent variables, and Λ is a $k \times m$ matrix of factor loadings that relate the observed variables to the latent variables.

In the present study, we used the *factanal* function of R to conduct an exploratory factor analysis with promax rotation. Guided by the results described in Supplementary Section 2.1, we tested factor solutions extracting up to three latent factors, retaining the highest dimensional solution where each factor explained at least 20% of the variance. As the three-factor solution did not meet this criterion (F1 = 43%, F2 = 26%, F3 = 18%), we selected the two-factor solution as the best exploratory factor model (Figure 2b).

In this two-factor solution, we found compelling evidence of approximate simple structure. Phenotypes principally loaded onto one of two latent genetic factors with negligible cross-loadings. The two correlated latent genetic factors explained 81.3% of the total genetic variance across phenotypes.

2.3 Structural equation modeling

Structural equation modeling is a statistical framework comprised of a diverse set of models and methods used to explain variance and covariance among sets of variables. While the background and many applications of structural equation modeling are extensive[7,8], the fundamentals as they relate to the Genomic SEM framework are briefly reviewed below.

Structural equation models can be represented in two sets of equations: the *measurement model*, which describes how observed variables relate to latent variables, and the *structural model*, which describes how latent variables relate to one another[6]. As in exploratory factor analysis, k observed variables are again described as linear functions of m continuous latent variables. In confirmatory factor analysis, this is referred to as the measurement model, which is still expressed as

$$y = \Lambda\eta + \varepsilon$$

with the same notation as described in Supplementary Section 2.2.

If theory is used to explain associations between latent variables, a structural model can then be specified to relate latent variables to each other via directed regression coefficients. The structural model can be expressed as

$$\eta = B\eta + \zeta$$

where B is a $m \times m$ matrix of regression coefficients that relate latent variables to one another and ζ is a $m \times 1$ vector of latent variable residuals. In this full structural equation model, the observed sample covariance matrix is represented by a set of parameters that relates observed variables to latent variables, and latent variables to each other in a series of linear equations.

Genomic SEM employs a two-stage SEM approach to model the genetic covariances between a set of phenotypes (*i.e.*, the observed phenotypes). Stage 1 consists of estimating the genetic covariance matrix and the sampling covariance matrix. Stage 2 consists of fitting a structural equation model that minimizes misfit between the model-implied and empirical genetic covariances.

In Stage 1, Genomic SEM uses a multivariable form of LD Score regression to estimate the empirical genetic covariance matrix (S) and its associated sampling covariance matrix (V_S). Here, S is a symmetric matrix of order k with SNP heritabilities on the diagonal and genetic covariances between phenotypes off the diagonal. Comprised of $k^* = \frac{k(k+1)}{2}$ nonredundant elements, S can be written as

$$S = \begin{bmatrix} h_1^2 & & & \\ \sigma_{g1.g2} & h_2^2 & & \\ \vdots & & \ddots & \\ \sigma_{g1,gk} & \sigma_{g2,gk} & \dots & h_k^2 \end{bmatrix}$$

To obtain unbiased estimates of standard errors and test statistics, Genomic SEM then constructs the asymptotic sampling covariance matrix of the LD Score regression estimates, V_S, by using all nonredundant elements in the S matrix. Here, V_S is a symmetric matrix of order $k^*$where the diagonal elements are sampling variances and the off-diagonal elements are sampling covariances. Thus, it can be written as

$$V_S = \begin{bmatrix} SE(h_1^2)^2 & & & & & & \\ cov(h_1^2, \sigma_{g_1,g_2}) & SE(\sigma_{g_1,g_2})^2 & & & & & \\ \vdots & \vdots & \ddots & & & & \\ cov(h_1^2, \sigma_{g_1,g_k}) & cov(\sigma_{g_1,g_2}, \sigma_{g_1,g_k}) & SE(\sigma_{g_1,g_k})^2 & & & & \\ \vdots & \vdots & \vdots & \ddots & & & \\ cov(h_1^2, h_j^2) & cov(\sigma_{g_1,g_2}, h_j^2) & cov(\sigma_{g_1,g_k}, h_j^2) & SE(h_j^2)^2 & & & \\ \vdots & \vdots & \vdots & & \ddots & & \\ cov(h_1^2, \sigma_{g_j,g_k}) & cov(\sigma_{g_1,g_2}, \sigma_{g_j,g_k}) & cov(\sigma_{g_1,g_k}, \sigma_{g_j,g_k}) & cov(h_j^2, \sigma_{g_j,g_k}) & SE(\sigma_{g_j,g_k})^2 & & \\ cov(h_1^2, h_k^2) & cov(\sigma_{g_1,g_2}, h_k^2) & cov(\sigma_{g_1,g_k}, h_k^2) & cov(h_j^2, h_k^2) & cov(\sigma_{g_j,g_k}, h_k^2) & SE(h_k^2)^2 \end{bmatrix}$$

The diagonal elements of V_S are then estimated with a jackknife resampling procedure following the original bivariate version of LD Score regression.

In Stage 2, Genomic SEM uses the S and V matrices from Stage 1 to estimate the parameters of the specified structural equation model using a weighted least squares (WLS) fit function, as detailed in Grotzinger et al. (2019). Notably, this method is capable of accounting for differences in GWAS sample size, which is ideal in the present study. Furthermore, the off-diagonal elements of V_S index the extent to which the sampling errors across input GWAS are correlated, which means that Genomic SEM, like LD score regression upon which it is based, is unbiased and robust to varying degrees of, or even complete, sample overlap.

2.3.1 Confirmatory factor analysis

Confirmatory factor analysis is a common application of structural modeling where theoretical models are used to explain the observed covariances among a set of observed variables. Here, we tested a series of competing models to identify the model that best fit the data, where good fit indicated that the specified latent variable structure adequately explained the observed genetic covariances among the set of observed variables.

Guided by the results described in Supplementary Sections 2.1 and 2.2, as well as psychiatric and psychometric theory, we tested a series of confirmatory factor models to identify the solution that best explained the observed genetic covariances among the set of discovery phenotypes. Specifically, we tested four models: (i) a single common factor model (*i.e.*, a *p* factor), (ii) a correlated factors model (iii) a correlated factors model with bipolar II disorder to cross-loading on both factors, and (iv) a correlated factors model with correlated residuals between bipolar I disorder and bipolar II disorder. Path diagrams for these models are presented in Figure S2. Unit variance identification was used to set the scale of the latent factors.

Model fit was assessed using conventional indices in structural equation modeling: the model χ^2 statistic, the Akaike information criterion (AIC), the comparative fit index (CFI), and the standardized root mean square residual (SRMR). All of these indices retain their standard interpretations within a Genomic SEM framework with the exception of the model χ^2 statistic [6]. In large samples, such as those used here, χ^2 tests are overpowered

and likely to be significant. As such, the model χ^2 statistic was used as a comparative measure of fit to evaluate competing models (akin to AIC), rather than a measure of statistical significance. For CFI and SRMR, values greater than .90 and less than .08, respectively, were considered reflective of good model fit[9].

Common factor model

As a baseline, we evaluated a common factor model with all eight phenotypes operating as indicators for a single latent factor. While easily interpretable, this particular model exhibited poor fit, as indicated by model fit indices ($\chi^2(20) = 1630.24$, AIC = 1662.24, CFI = .99, SRMR = .20). Inspection of the observed and model implied genetic correlation matrices indicated that the common factor model implied that genetic correlations between schizophrenia, schizoaffective disorder, bipolar I disorder, and bipolar II disorder were severely downwardly biased. Moreover, the genetic correlations between psychiatric symptoms and disorders were modestly upwardly biased in the common factor model.

Correlated factors model

Preliminary results described in Supplementary Sections 2.1 and 2.2 suggested the promise of a two-factor model, where phenotypes loaded onto two distinct-but-correlated latent genetic factors. As an initial test of this model, we estimated a simple correlated factors model with no cross-loadings and no correlated residuals. While this model had better fit than the common factor model, some model fit indices were still suboptimal ($\chi^2(19) = 608.97$, AIC = 642.97, CFI = .99, SRMR = .11). We next fit a model allowing bipolar II disorder to cross-load onto both factors. This model also showed good fit, as indicated by model fit indices ($\chi2(18) = 390.93$, AIC = 426.93, CFI = .99, SRMR = .08), but the cross-loading resulted in markedly lower loadings for bipolar II disorder (.51 and .43 for F1 and F2, specifically). Finally, we fit a correlated factors model that estimated the correlation between residual variance in bipolar I disorder and bipolar II disorder. This model fit the data best, closely approximating the observed genetic covariance matrix ($\chi2(18) = 496.16$, AIC = 532.16, CFI = .99, SRMR = .06).

While all variations of the correlated factors model showed improved fit over the common factor model, we identified the model that included correlated residuals as the best fitting model. Notably, this model provided a parsimonious and easily interpretable factor structure that simultaneously minimized the standardized difference between the observed and predicted genetic correlations. Inspection of the observed and model implied genetic correlation matrices indicated that the final correlated factors model fit the data substantially better than the common factor model because it appropriately accounted for different patterns of covariance by segregating the phenotypes into two separate-but-correlated latent factors (Figure S3).

2.3.2 Genetic correlation

Structural equation models can also be used to estimate the genetic correlation between an unobserved latent factor and an observed exogenous phenotype not included in the model. Indeed, this method is preferable to using bivariate LD score regression, as it based on the genetic covariances directly rather than the estimated SNP effects, which may not be mediated by the latent factor(s) (see Supplementary Section 2.5 for more on heterogenous SNP effects). To estimate genetic correlations between a latent factor and an observed exogenous phenotype, we first created a single-item quasi-latent factor for the exogenous phenotype, and fixed the residual variance for the phenotype to zero. We then estimated the correlation between our latent factors and the quasi-latent factor for the phenotype of interest.

2.3.3 Multivariable genetic regression

The approach described in Supplementary Section 2.3.2 can be extended to conduct multivariable genetic regression, which yields estimates of genetic associations between two variables after accounting for relationships with additional variables in the model (*i.e.*, partial genetic correlations). Here, this is done by

regressing the exogenous phenotype onto F1 and F2 while simultaneously estimating the genetic correlation between the two latent genetic factors.

2.4 Multivariate genome-wide association analyses

After identifying a confirmatory factor model that best explained the observed genetic covariances among the phenotypes, we conducted a multivariate GWAS by estimating the individual SNP effects on each latent factor in the model. A brief overview of this method is provided below.

To estimate the effect of SNP j on F1 and F2, individual SNP effects are included in both the genetic covariance matrix and the sampling covariance matrix. This is accomplished by expanding the genetic covariance matrix to include covariances between SNP j and the latent genetic components of each phenotype, g_1 through g_k.

$$S = \begin{bmatrix} \sigma^2_{SNP} & & & \\ \sigma_{SNP,g_1} & h^2_1 & & \\ \sigma_{SNP,g_2} & \sigma_{g_1,g_2} & h^2_2 & \\ \sigma_{SNP,g_k} & \sigma_{g_1,g_k} & \sigma_{g_2,g_k} & h^2_k \end{bmatrix}$$

The associated sampling covariance matrix, V_S, then includes the following: (i) the sampling variances and sampling covariances of the SNP heritabilities and genetic covariances, (ii) the variance of SNP j as derived from reference panel data, and (iii) the sampling covariances of the SNP-genotype covariances. Finally, Genomic SEM is used to estimate m models to obtain GWAS summary statistic for the latent factors, where m is the number of SNPs present across all included summary statistics.

Note that unit loading identification is used to set the scale of latent factors for models including SNP effects. This is a difference from the structural equation models without SNP effects, where unit variance identification is used to facilitate easy interpretation of factor loadings. This is done for two reasons. First, if the variance of the factor were set to 1, the inclusion of a SNP as a regressor technically changes the variance of the latent factor to be 1 plus the variance explained by the SNP. Second, the use of unit variance identification scales SNP effects as if they were for a phenotype that was entirely heritable (*i.e.*, $h^2_{SNP} = 1$). This distinction does not change the ratio of effect estimates to standard errors, but it does potentially complicate comparison to other GWAS results. Thus, we find that unit loading identification is the most appropriate method to scale latent factors in models that include SNP effects. Here, we set the scale of F1 and F2 by fixing the factor loadings of psychotic symptoms and schizophrenia, respectively.

2.5 Heterogeneity tests

It is possible that SNP effects might vary across each indicator and not act entirely through the common latent variable. To evaluate this potential heterogeneity in SNP effects, we computed genome-wide Q_{SNP} statistics, which are χ^2-distributed test statistics estimated for each SNP in the multivariate GWAS. As described by Grotzinger and colleagues[6], larger values for Q_{SNP} reflect a violation of the null hypothesis that the SNP acts entirely through the latent factor(s).

2.6 Effective sample size

While it can be difficult to estimate effective sample size for a given SNP in a latent factor model, we were able to produce reasonable estimates of effective sample size for the overall multivariate GWAS under a set of reasonable assumptions. First, we assume that the per-allele effect of SNP j on the standardized phenotype is very small, such that it follows

$$\beta_j = \frac{Z_j}{\sqrt{n_j \times 2 \times MAF_j\left(1 - MAF_j\right)}}$$

where Z is the Z statistic, n is the unknown effective sample size that we seek to estimate, and MAF is the minor allele frequency of SNP j. Note that the variance of SNP j (σ_j^2) is estimated as $2 \times MAF_j\left(1 - MAF_j\right)$. Therefore, if we know the effect and MAF of that SNP, then we can estimate its effective sample size by solving for n_j.

$$\frac{\beta_j}{Z_j} = \frac{1}{\sqrt{n_j \times \sigma_j^2}}$$

$$\frac{Z_j}{\beta_j} = \sqrt{n_j \times \sigma_j^2}$$

$$\left(\frac{Z_j}{\beta_j}\right)^2 = n_j \times \sigma_j^2$$

$$n_j = \frac{(Z_j/\beta_j)^2}{\sigma_j^2}$$

We note that when the phenotype is a latent factor, the choice of scaling the factor will have a nontrivial effect on the estimate of n_j. Here we scale the latent genetic factors with unit loading identification, such that n_j can be intuitively interpreted as the effective sample size in the units of the standardized reference phenotype (As indicated in 2.4, we set the scale of F1 and F2 by fixing the factor loadings of psychotic symptoms and schizophrenia, respectively). If we were to scale the latent genetic factors with unit variance identification, the effective sample size would be interpreted relative to a factor that is 100% heritable, and n_j would be unintuitively very small (because, ceteris paribus, highly heritable phenotypes require smaller sample sizes to detect genetic associations).

This formula will typically produce reasonable estimates of n_j when the factor is scaled using a unit loading identification strategy, but it can be prone to error for SNPs with low MAF. Here, we set a lower and upper MAF limit of approximately 10% and 40%, respectively, when estimating effective N for the overall multivariate GWAS results (N_{eff}). Following this, we estimate that N_{eff} is approximately equal to the mean n_j for m SNPs with a MAF between a and b. This can be expressed as

$$N_{eff} \approx \frac{1}{m} \sum_{MAF=a}^{b} n_j$$

Here, we apply this to the results for the results for F1 and F2 and estimate that the effective N for each phenotype is 377,518 and 51,276, respectively. We note that this calculation is robust to sample overlap in the multivariate GWAS, as Genomic SEM accounts and corrects for such overlap.

We note that with an effective sample size, it is possible to backout an estimate of genetic variance that is, in one sense, conceptually analogous to SNP heritability in that they reflect the scale of SNP effects for a GWAS

target. However, as there is no information about phenotypic variance of the latent genetic factors, it should not be interpreted as a heritability estimate. Rather, these genetic variance estimates are only useful as an additional metric for comparing GWAS results when paired with effective sample size. Here, the latent factors F1 and F2 have genetic variance estimates of 6% (SE = .28%) and 56% (SE = 2.29%) respectively. The genetic variance estimates for F1 and F2 differ because of the differing SNP heritability estimates of their underlying indicators, with lower heritability estimates observed for self-report symptoms than for clinically-defined disorders. The greater proportion of non-genetic variance in self-report symptoms might be due to greater influence of environmental variation and/or greater unreliability of measurement.

3 References

1. Muthén, L.K., and Muthén, B. (2017). Mplus User's Guide: Eighth Edition (Muthén & Muthén).

2. Curran, P.J., Hussong, A.M., Cai, L., Huang, W., Chassin, L., Sher, K.J., and Zucker, R.A. (2008). Pooling data from multiple longitudinal studies: the role of item response theory in integrative data analysis. Dev. Psychol. *44*, 365–80.

3. Abraham, G., Qiu, Y., and Inouye, M. (2017). FlashPCA2: principal component analysis of Biobank-scale genotype datasets. Bioinformatics *33*, 2776–2778.

4. Winkler, T.W., Day, F.R., Croteau-Chonka, D.C., Wood, A.R., Locke, A.E., Mägi, R., Ferreira, T., Fall, T., Graff, M., Justice, A.E., et al. (2014). Quality control and conduct of genome-wide association meta-analyses. Nat. Protoc. *9*, 1192–212.

5. Karlsson Linnér, R., Biroli, P., Kong, E., Meddens, S.F.W., Wedow, R., Fontana, M.A., Lebreton, M., Tino, S.P., Abdellaoui, A., Hammerschlag, A.R., et al. (2019). Genome-wide association analyses of risk tolerance and risky behaviors in over 1 million individuals identify hundreds of loci and shared genetic influences. Nat. Genet. *51*, 245–257.

6. Grotzinger, A.D., Rhemtulla, M., de Vlaming, R., Ritchie, S.J., Mallard, T.T., Hill, W.D., Ip, H.F., Marioni, R.E., McIntosh, A.M., Deary, I.J., et al. (2019). Genomic structural equation modelling provides insights into the multivariate genetic architecture of complex traits. Nat. Hum. Behav. *3*, 513–525.

7. Loehlin, J.C., and Beaujean, A.A. (2016). Latent variable models: an introduction to factor, path, and structural equation analysis (Taylor & Francis).

8. Kline, R.B. (2015). Principles and practice of structural equation modeling (Guilford publications).

9. Hu, L., and Bentler, P.M. (1999). Cutoff criteria for fit indexes in covariance structure analysis: conventional criteria versus new alternatives. Struct. Equ. Modeling *6*, 1–55.